Control System Design of Tilt Rotor Unmanned Aerial Vehicle (UAV)

Debabrata Mahapatra (109EE0277)

Department of Electrical Engineering
National Institute of Technology Rourkela

Control System Design of Tilt Rotor Unmanned Aerial Vehicle (UAV)

A Thesis submitted in partial fulfillment of the requirements for the degree of

Bachelor of Technology in "Electrical Engineering"

By

Debabrata Mahapatra (109EE0277)

Under guidance of

Prof. B.D. Subudhi

Department of Electrical Engineering

National Institute of Technology

Rourkela-769008 (ODISHA)

May-2011

DEPARTMENT OF ELECTRICAL ENGINEERING

NATIONAL INSTITUTE OF TECHNOLOGY, ROURKELA

ODISHA, INDIA-769008

CERTIFICATE

This is to certify that the thesis entitled "**Control System Design of Tilt Rotor Unmanned Aerial Vehicle (UAV)**", submitted by **Debabrata Mahapatra (Roll. No. 109EE0277),** in partial fulfilment of the requirements for the award of **Bachelor of Technology** in **Electrical Engineering** during session 2012-2013 at National Institute of Technology, Rourkela. A bonafide record of research work carried out by them under my supervision and guidance.

The candidates have fulfilled all the prescribed requirements.

The Thesis which is based on candidates' own work, have not submitted elsewhere for a degree/diploma.

In my opinion, the thesis is of standard required for the award of a bachelor of technology degree in Electrical Engineering.

Place: Rourkela

Dept. of Electrical Engineering **Prof. B.D. Subudhi**

National institute of Technology

Rourkela-769008

ACKNOWLEDGEMENTS

On the submission of my thesis entitled "**Control System Design of Tilt Rotor Unmanned Aerial Vehicle (UAV)**", I would like to extend my gratitude & my sincere thanks to my supervisor **Prof. B.D. Subudhi**, Department of Electrical Engineering for his constant motivation and support during the course of my work in the last one year. I truly appreciate and value his esteemed guidance and encouragement from the beginning to the end of this thesis. His knowledge and company at the time of crisis would be remembered lifelong.

I am very thankful to **Prof. B.Chitti Babu** for his valuable suggestions and comments during this project period.

I am very thankful to our teachers **Prof. Susovan Samanta** and **Prof. Subhojit Ghosh** for providing solid background for my studies and research thereafter. They have been great sources of inspiration to me and I thank them from the bottom of our hearts.

At last but not least, I would like to thank the staff of Electrical engineering department for constant support and providing place to work during project period. I would also like to extend my gratitude to my friends who are with me during thick and thin.

Debabrata Mahapatra

B.Tech (Electrical Engineering)

Dedicated to

My beloved parents

ABSTRACT

Unmanned Aerial Vehicles (UAVs) are those flying aircrafts that run without any humans being onboard. They are controlled either by an onboard computer or remote controllers. Utilizing UAVs for intelligence, surveillance, and reconnaissance (ISR) is beneficial in both military and civil applications. The various usages of these kinds of aircrafts are in different military missions such as battle damage assessment, communications relay, minesweeping, hazardous substances detection. However they can be used in other than military missions like monitoring the deployment of ballistics and projectiles while testing and locating there fall of shot. Aircrafts that are able of hovering and vertical flying can be used for this type of specific assignment. Having vertical take-off and landing (VTOL) capabilities and fast gliding provisions, tiltrotor aircraft is a very handy model which is perfectly compatible for many applications, which a nominal RC glider or a hovering helicopter may not perform efficiently. Combining the property of fast gliding of RC gliders and stable hovering capabilities of RC helicopter/quad copter, the tiltrotor mechanism works satisfactorily in spite of its complex flight dynamics. This mechanism presents a challenge for flight control designers and handling qualities engineers. Achieving consistent handling qualities and dynamic stability throughout an operational flight envelope is difficult since the aircraft's flight dynamics change significantly at different operating conditions (e.g. speed, attitudes, etc.) and configurations (e.g. helicopter mode, conversion mode or airplane mode). The requirement to meet both helicopter and fixed wing flying qualities specifications always results in substantial cost and time. Development of integrated methods for flight control design and handling qualities analysis could greatly enhance the future of tiltrotor aircraft and can widen the sphere of UAV applications.

CONTENTS

LIST OF FIGURES

Chapter 1
INTRODUCTION

1.1 RATIONALE

Dynamic stabilization and Handling qualities are the characteristics of an aircraft (UAV) that govern the ease and precision with it is able to perform the tasks required. Handling qualities requirements are intended to assure that there is no limitation on flight safety or on the capability to perform particular tasks resulting from excessive application workload. In order to meet those requirements, a suitable Flight Control System (FCS) is needed. Therefore, Flight Control design plays an important role to ensure the aircraft is compatible to do particular job [1].

The UAVs are basically designed to carry out specific missions. Generally, there are three design options that the designers have: fixed-wing type, vertical take-off and landing (VTOL) type and the design that mix between the two.

One of the important aspects that shape the UAV design is the mission requirement. Whilst each type of UAV has its own advantages, the one which has the VTOL capability offers greater operational flexibility. VTOL UAVs have advantages over fixed-wing UAVs in several ways: the ability of the UAV to take off and land vertically means that a runway is not necessary, and in fact these vehicles can be easily deployed and recovered from relatively small areas. The vehicle can also maneuver freely in three dimensions thus making it well suited for flying through cluttered spaces such as forests or any built-up environment.

1.2 MOTIVATION

Defense Research Development Organization (DRDO) Chandipur test fires various types' ballistics and projectiles of various ranges. The fall of shot at the deployment point is measured by surveying equipment which is fixed on Observation Points (OP), using triangulation method.

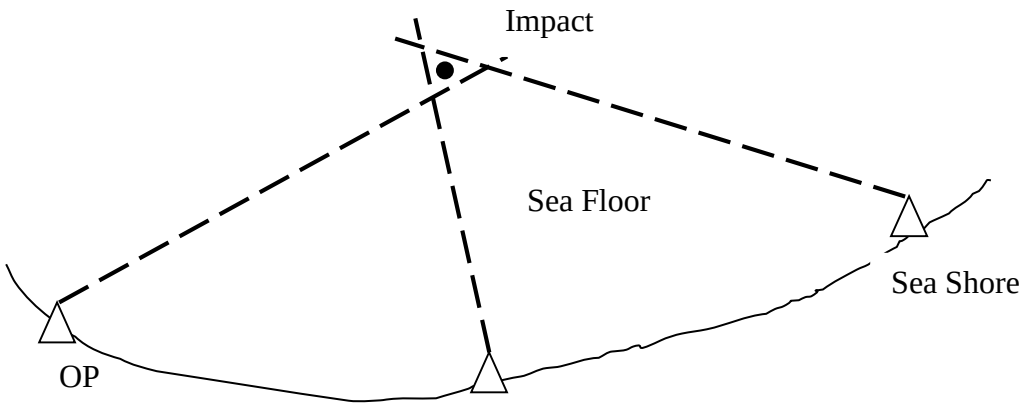

Figure 1-1 Triangulation Method for Observation of Fall of shot

Usually, operator moves the equipment after he sees the impact (Impact point is about 2000m to 3000m from Observation Post). Hence locating the fall of shot after impact becomes the job of expert; which has good amount of possibility of escaping the exact location of impact. A large safety distance is required to be maintained between impact region and observation posts. This results in reduction of accuracy.

So the task is to develop a device which can attain height and can monitor the event and also locate the fall of shot with great accuracy with the measuring instruments onboard and communicate with the ground station. For doing that the hovering device is needed to have very good stability and the agility to change its observation point quickly when the range of missile varies as well. And the tiltrotor UAV is best suited for their requirement. The challenge in flight control design is to achieve desired handling qualities over the entire flight envelope. The tiltrotor has a wide range of configurations. Not only do the aircraft flight dynamics vary significantly for different operating conditions, but also control characteristics change during the conversion from airplane-like configuration to helicopter like configuration.

1.3 PROJECT OBJECTIVES

Accurate system modelling is an essential part of controller design. And sometimes the case is so when accurate mathematical model leads to very complex controller design. On the other hand if we choose to use conventional control techniques by simplifying the system model then hardware complexity of the system is increased exponentially. That is why there is always a trade of to make between system modelling and performance. So the purpose of this research is to show the advantages of choosing modern control techniques to have better handling quality performance with less hard ware complexities.

So the objective here is to

a) Development of the mathematical model of the aircraft by considering Coriolis effects.

b) Development of Controller by using reducing the system dynamics.

c) Simulation of the reduced system dynamics

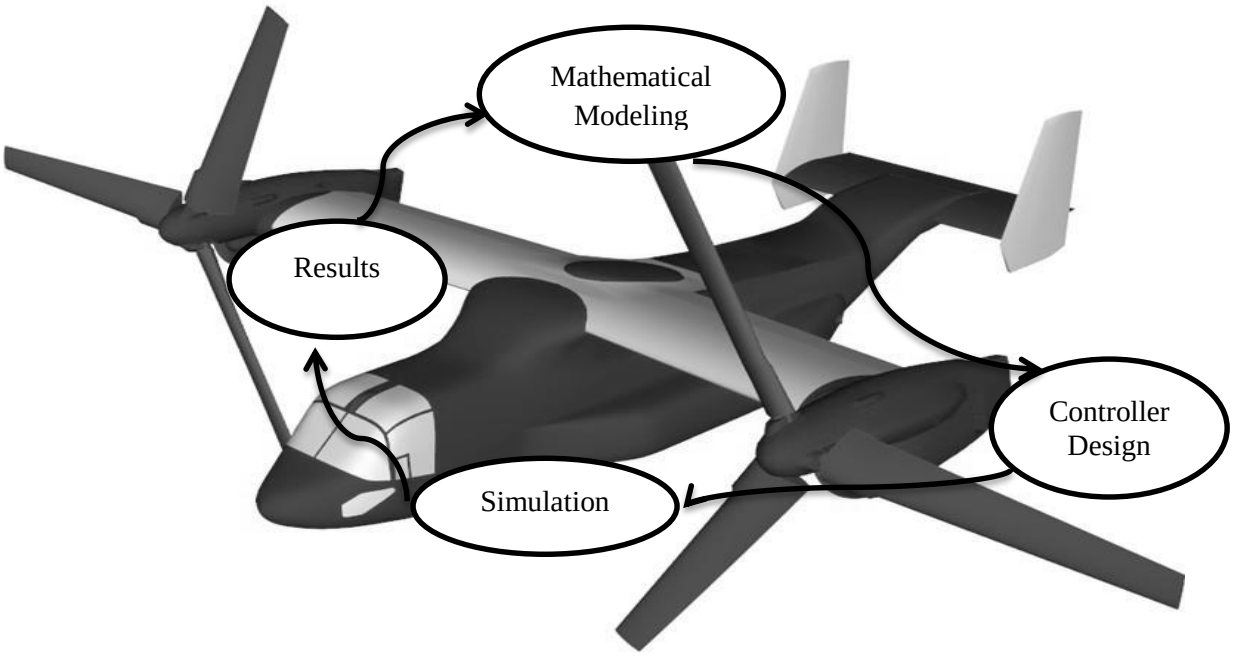

Figure 1-2 Road map for fly-by-wire flight-control system development and integration [11]

Chapter 2

THEORETICAL BACKGROUND AND LITERATURE OVERVIEW

2.1 INTRODUCTION

This chapter begins with a broad overview of the UAV flight missions where VTOL capability is required. Then, we focus on a more specific flight missions where success relies on a UAV configuration with the following characteristics: VTOL capability, and high speed capability. Several existing tiltrotor UAVs were reviewed, followed by a discussion on the challenges in developing an autonomous flight control system for such a vehicle. After that basic mechanisms of flight control are briefed. A brief review of the techniques already adopted by various researchers is given.

2.2 NEEDS AND CHALLENGES FOR VTOL UAVS

Many UAVs that have been in service, either in military or civil applications, are of fixed-wing type. Some of these UAVs that serve the U.S. military are MQ-Predator, RQ-2 Pioneer, and, RQ-5 Hunter, and RQ-4 Global Hawk as shown in Figure 2.1. The physical appearance and operation principles of these vehicles very much resemble an ordinary aircraft. In particular, a runway is needed for take-off and landing, and it means a large flat operational area is required.

(a) (b)

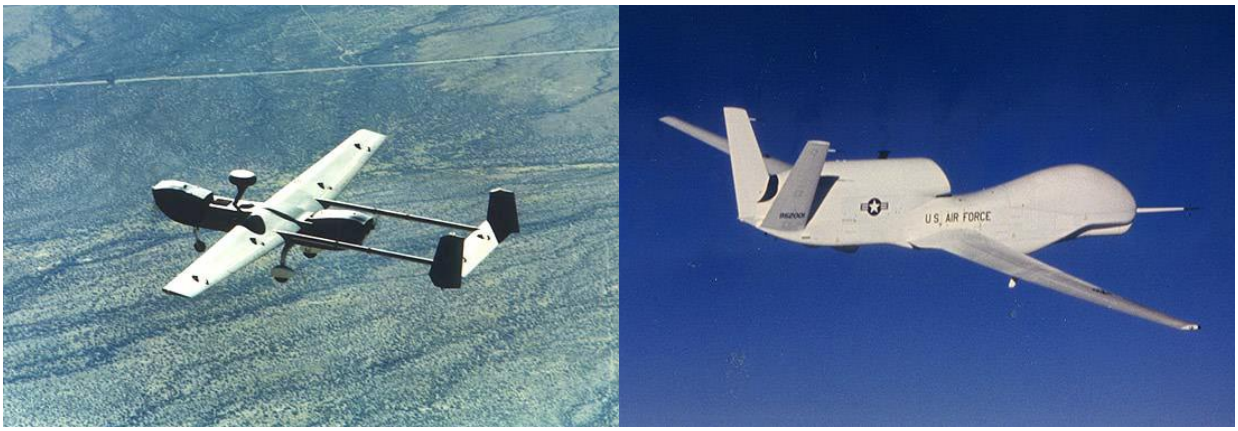

(b) (d)

Figure 2-1 Fixed-wing UAVs: (a) Predator [11], (b) Pioneer [12], (c) Hunter [13], (d) Global Hawk [14]

However, in many circumstances the use of a runway for UAVs is impractical. For example in military applications, conventional runways are often unavailable adjacent to the operational military zone, or the available runways are only for larger aircraft. In shipboard based UAVs operations, the problem becomes worse since the available space for the onboard runway is further reduced. While some of the military ships may have limited space for shipboard recovery, this available space is usually fully used by larger manned aircraft. To address this shipboard problem, expensive recovery systems are often employed such as recovery nets, parachute systems, deep stall landing, and in flight arresting devices [3]. Another critical problem associated with fixed-wing UAVs is that these vehicles are often unsuitable to operate effectively in confined airspace and area. This becomes evident in urban settings where the use of a runway is not possible, and UAVs are usually required to fly at a relatively low speed and altitude.

The limited operational flexibility of fixed-wing UAVs has led to the development of VTOL UAVs. The term VTOL is self-explanatory. By having VTOL capability, the aforementioned problems of runway needs and shipboard recovery systems are addressed. The unneeded runway means the vehicle has greater freedom in its operational environment. As such,

this type of UAV can be deployed from virtually any place, as long as minimal clear space is available for take-off and landing. Furthermore, VTOL UAVs are able to hover, which is an important flying characteristic in confined territory. In general, the VTOL UAV is acquiring the performance and motion flexibility of a helicopter. Being able to hover and land in small areas makes a VTOL UAV valuable for surveillance tasks, in that it can land in an area of interest, shut off the engine, becoming a stationary sensor platform until it needs to fly again. Among the early designs of a VTOL UAV is the QH-50 shown in Figure 2.2(a). Developed by the US Navy, this remotely piloted UAV was designed for anti-submarine warfare attack capabilities through the

(a) (b)

Figure 2-2 Rotorcraft VTOL UAV: (a) Coaxial rotors [15], (b) Single rotor

use of a drone torpedo delivery platform. The principal benefit of the coaxial rotor configuration is it offers the same aerodynamic efficiency and controllability for flight in any direction.

In this rotor configuration, the dissymmetry of lift on the first rotor is cancelled by the corresponding increase in lift on the other rotor. This would result in a vehicle that can fly faster than a single-rotor design, and is more stable in extreme parts of the flight envelope. However, the coaxial flapping rotor design increases mechanical complexity of the rotor hub, and also gives weight penalty. The linkages and swash plates for two rotor discs need to be assembled around the rotor shaft, which itself is more complex because of the need to drive two rotor discs in opposite

directions. These disadvantages are also true for the single rotor unmanned helicopter such as the UAV shown in Figure 2.2(b). The complexity in the mechanical linkages is even further increased in the single rotor UAV. This is because the blades have to be flapped in order to solve the dissymmetry of lift on the rotating blades, and usually needs an extra tail fan to cancel the torque developed by the main rotor. Adapting a helicopter configuration also means that the UAV has to use a very complicated cyclic and collective rotor control. A study by the US Marine Corps has concluded that single rotor unmanned helicopters are more expensive, less reliable, and offered no advantage to manned helicopters [10].

2.3 DEMANDS FOR TILTROTOR UAVs

Other than the design complexity in existing helicopter-type UAVs, a significant weakness in helicopter-like vehicles is they suffer from low speed forward flight, in addition to the configuration disadvantages that we have discussed above. Tilt-rotor UAV overcomes the low speed performance by converting to high speed airplane mode once the take-off is completed. A major drawback in this configuration is the need for the rotor and wing to tilt, adding to the design complexity of mechanical linkages and control. The tail-sitter has the same ability to reach high speed flight, but this is achieved by rotating the whole body horizontally. The tail sitter concept gives a very promising solution for VTOL UAV configurations. It captures both VTOL and fixed-wing capabilities. Nevertheless, the bare propeller of this configuration is prone to endangering the operator and creates noise.

2.4 TILTROTOR UAV

As discussed above the dual use of a tiltrotor aircraft is illustrated in Figure 2.3. This model, XV-15, tiltrotor project was aimed to meet both civil and military needs by NASA-Army-Bell cooperation [4].

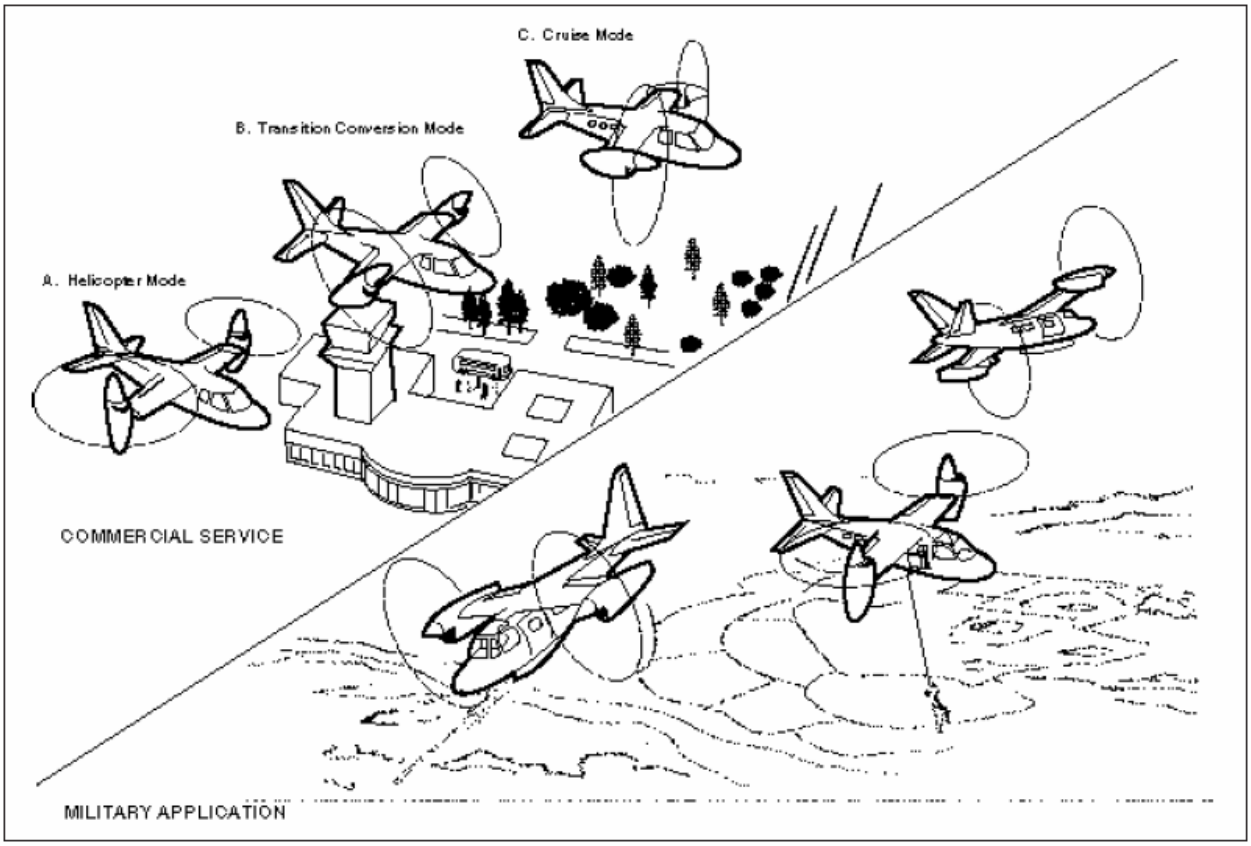

Figure 2-3 Illustration from 1974 Tiltrotor Research Project Plan [4]

This is capable of controlling roll, yaw, pitch and thrust in both modes, i.e. helicopter and airplane. The various collective pitch configurations for the 3 control movements are illustrated in Figure 2.4. In the helicopter mode, the controls apply collective or cyclic blade pitch changes to the rotors to produce control moments and forces. Fore and aft cyclic pitch provides longitudinal control and, differential longitudinal cyclic pitch produces directional control. Collective pitch is used for vertical control, and differential collective pitch is used for lateral control [4].

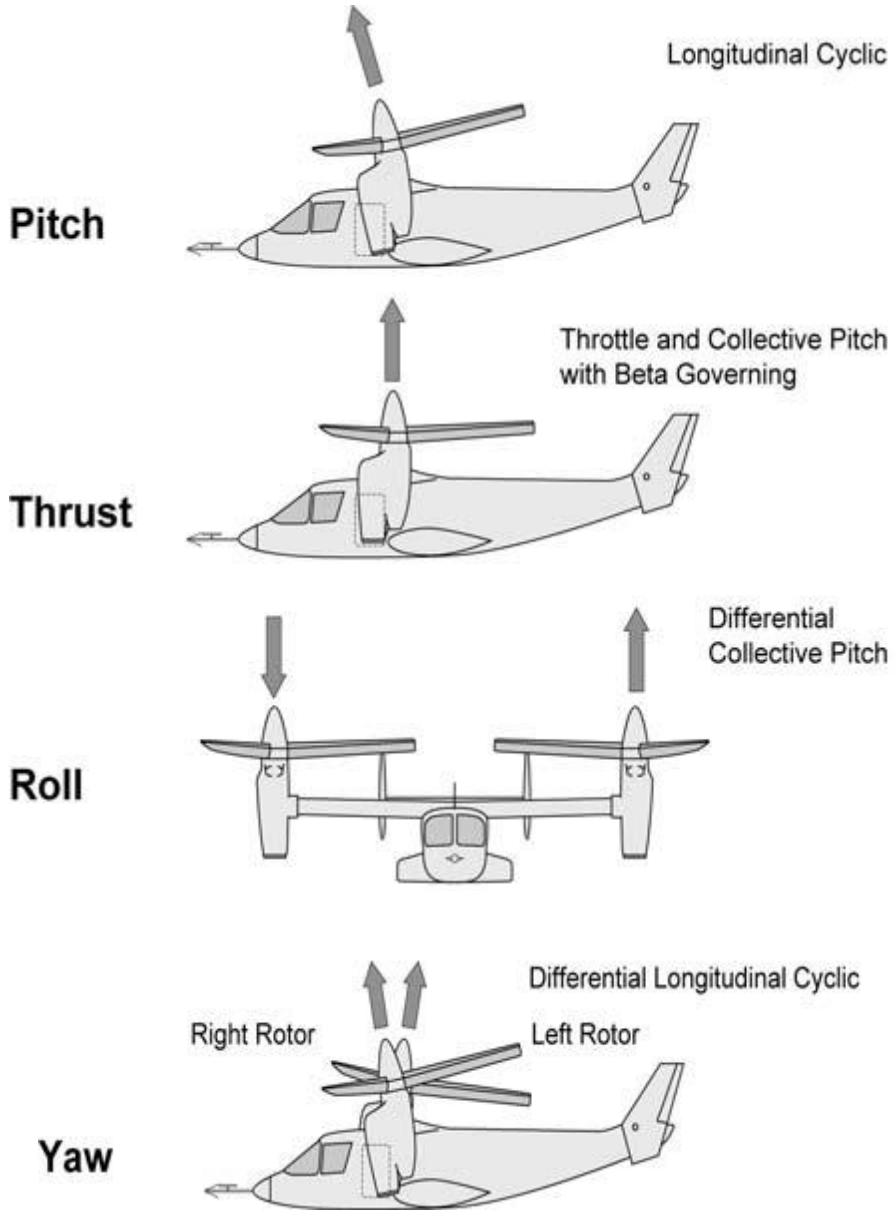

Figure 2-4 Control functions in helicopter mode [10]

In airplane mode, when the nascelles are tilted fully forward, the controls apply commands to ailerons, elevators and rudders (fixed wing control surfaces) to produce flight path control moments and forces as a conventional airplane. The differential cyclic pitch and differential collective pitch of rotors are not used. Only collective pitch that is used to control forward thrust [4]. The control functions in airplane configuration are illustrated in Figure 2.5.

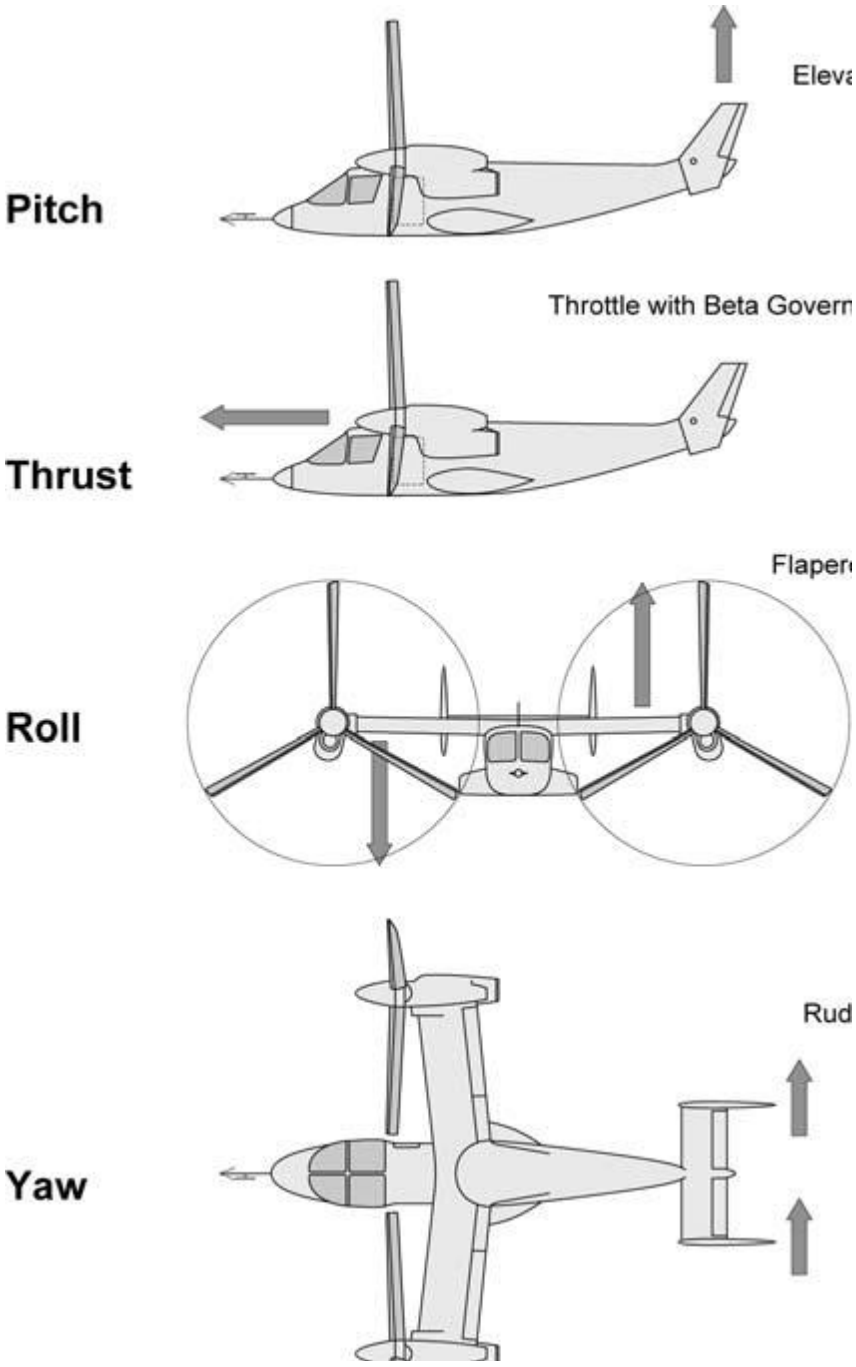

Figure 2-5 Airplane mode control functions [10]

In conversion mode, controls can be made suitable for a range of airspeeds, nascelle angles and fuselage attitudes.

2.5 LITERATURE SURVEY

Dynamic model inversion is a popular feedback linearization method for achieving consistent response characteristics. It has been applied to several types of aircraft. Its capabilities have been demonstrated for both helicopter and fixed-wing aircraft [5, 6].

In tiltrotor aircraft, there is little information about the flight control systems used in the real vehicle (XV-3, XV-15, V-22 Osprey, etc.) in the public domain. Calise and Rysdyk did researches on adaptive flight control using model inversion control with neural networks for XV-15 simulation model [6, 7, and 8]. Their controller showed good results in tracking commanded attitudes for the tiltrotor model in helicopter mode. By using model predictive control concept the design of XV-15 Flight Control System was successfully performed [1]. It was proven to have controller achieved performance and satisfied stringent robustness and stability requirements for XV-15 in airplane configuration. Walker and Voskuijl in University of Liverpool (UoL) applied $H_{infinity}$ to design a longitudinal axis augmentation system for XV-15 tiltrotor aircraft in airplane mode [9].

Chapter 3
MATHEMATICAL MODELING OF TILTROTOR UAV

The tiltrotor model investigated in this study was based on V-22 Osprey aircraft. The accurate modeling of a large flight envelope is difficult. But by mathematical modeling, the linear models at trim points are calculated. The required physical parameters for mathematical modeling are generally gathered from the time response data obtained from the test.

The tiltrotor (figure 3-2) model is composed of a fuselage, two wings, nacelles mounted at the wings tips, rotors mounted in front of the nacelles and a horizontal stabilizer and two vertical stabilizer. All components of the aircraft are rigid. The rotors have three blades fixed to the shaft by a pitch bearing. The pitch angles of rotor blades are controlled by swash-plates for constant (collective) and harmonic (cyclic) components. Horizontal stabilizer, vertical stabilizer and the tail are combinedly called as empennage.

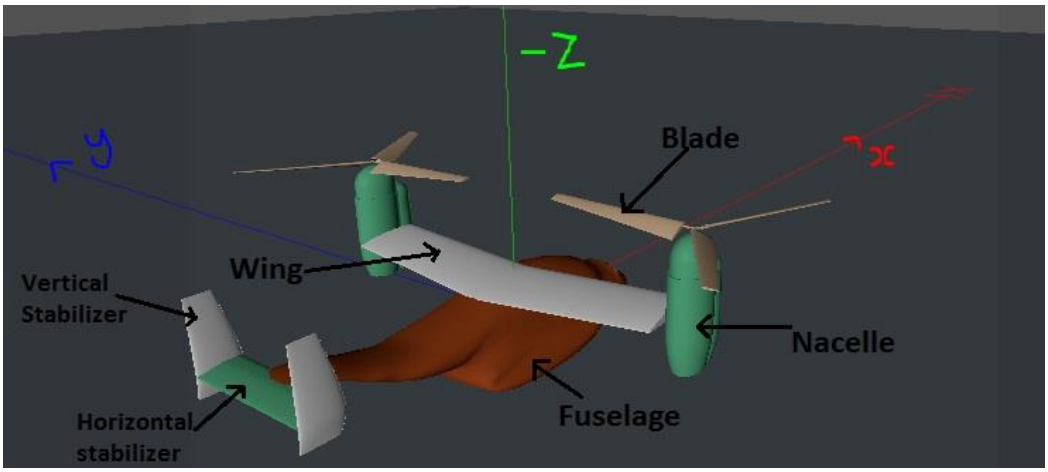

Figure 3-1 Configuration of tiltrotor

3.1 REFERENCE FRAMES

In every dynamics problem, there must be an inertial reference frame, either explicitly defined, lurking implicitly in the background. This frame is fixed, or in uniform rectilinear

translation relative to the distant stars. For the mathematical modeling we need to define the reference frame based on which the modeling will be done.

3.1.1 Earth or Ground Reference frame ($O_g x_g y_g z_g$)

Since this project is relevant to small range flights and subsonic speed the rotation of earth can be neglected and earth's surface can be considered as an inertial frame as shown in Figure 3-3.

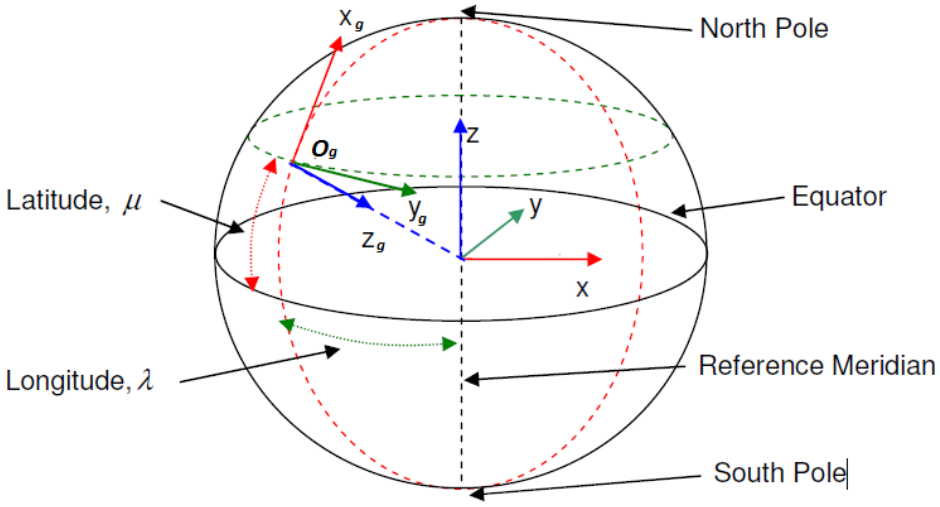

Figure 3-2 Earth Frame

O_g can be the launching point of vehicle, having z_g axis directed vertically downward from the surface to the center of the earth, $x_g y_g$ axis is the local horizontal plane, x_g pointing north and y_g pointing east.

3.1.2 Vehicle Carried or Gravity Reference frame ($O_G x_G y_G z_G$)

This frame has origin attached to the vehicle at the origin of fuselage. z_G axis is directed downward, i.e. same direction of the local g(gravitational acceleration) vector. The other axes are directed parallel to the earth frame's corresponding axes. Since the origin of the earth is close

proximity to the vehicle, the curvature of the earth is considered to be negligible, with flat earth approximation. This is illustrated in Figure 3-3.

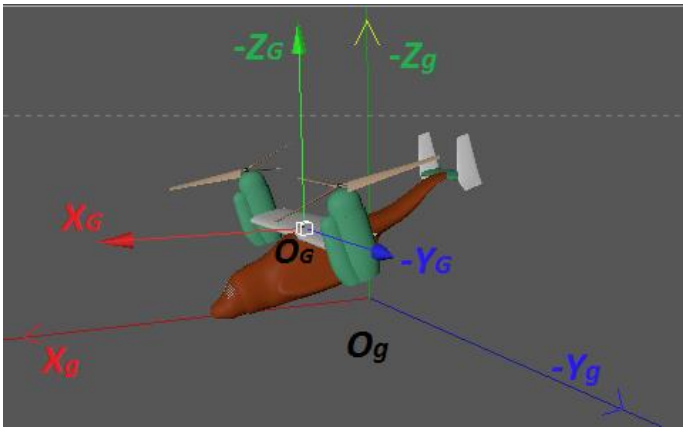

Figure 3-3 Gravity Frame

3.1.3 Body-fixed Frame or Fuselage Frame of Reference ($O_p x_p y_p z_p$)

Any set of axes fixed in a rigid body is a body–fixed reference frame. Looking from the cockpit, the nose of the aircraft points the x_p axis, right side points y_p axis and z_p points downward according to right hand rule. The center O_p of the system is placed in the point, where rotor shaft intersects with the fuselage plane of symmetry. O_p Fuselage center is same as O_G. This illustrated in figure 3-4.

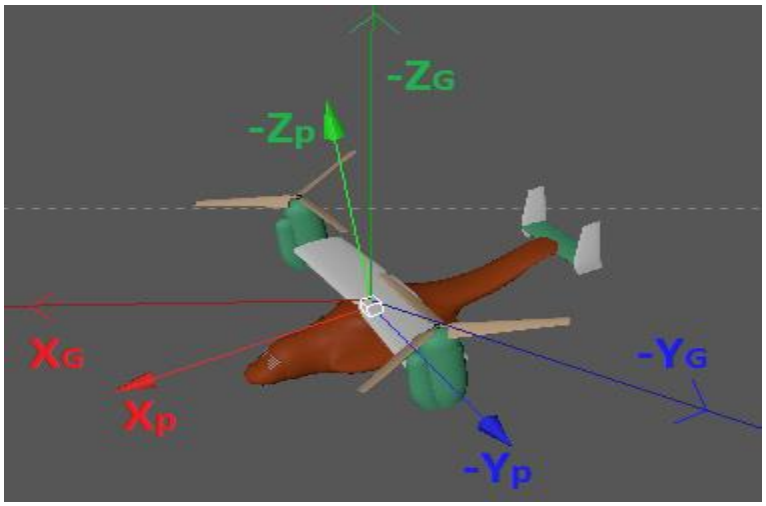

Figure 3-4 Body-Fixed Reference Frame

3.1.4 Nacelle Frame of Reference ($O_{n()}x_{n()}y_{n()}z_{n()}$)

$O_{nr}x_{n}y_{nr}z_{nr}$ = Right Nacelle Frame

$O_{nl}x_{nl}y_{nl}z_{nl}$ = Left Nacelle Frame

The nacelle, when points upward its $x_{n()}$ axis faces towards the vertical up. Nacelle is moved a tilt angle $\boldsymbol{\tau}$ about it's $y_{n()}$ axis for the control purposes. This is illustrated in Figure 3-5.

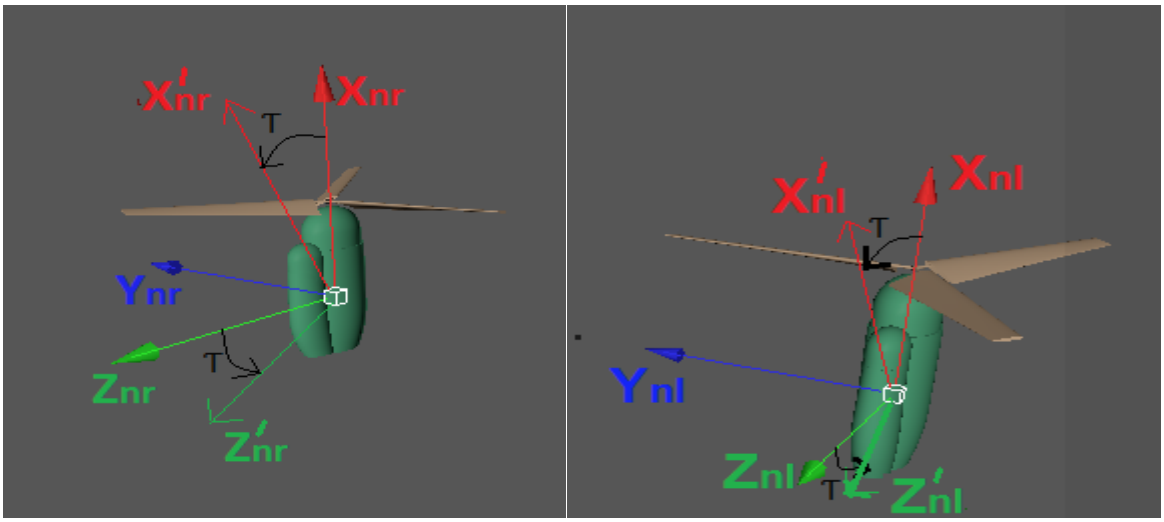

Figure 3-5 Nacelle Reference Frame

3.1.5 Hub Frame of Reference ($O_{h()}x_{h()}y_{h()}z_{h()}$)

$O_{hr}x_{hr}y_{hr}z_{hr}$ = Right Hub

$O_{hl}x_{hl}y_{hl}z_{hl}$ = Left Hub

When rotor disk is in horizontal plane the axis facing towards empennage is $x_{h()}$ axis. The Rotor disk area axis is the $z_{h()}$ axis. And the left out axis according to left hand finger rule is the $y_{h()}$ axis. Rotor disk is rotated about its $z_{h()}$ axis. While the $\boldsymbol{\tau = 90^{\circ}}$, i.e. the rotor is in vertical plane, looking from the empennage the right rotates clockwise and the left rotor anti-clockwise. This is illustrated in Figure 3-6.

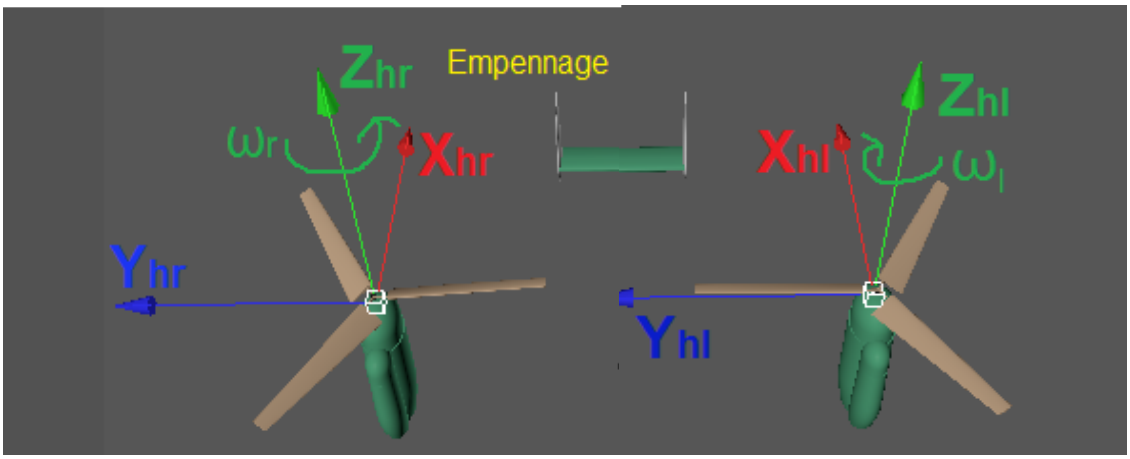

Figure 3-6 Hub Frame of Reference

3.2 ORIENTATION OF AIRPLANE w.r.t. INERTIAL FRAME: EULER ANGLES

- Translate the inertial frame and make it coincide with the CG.
- Make the sequential transformation of this frame so as to make it parallel to the body frame.

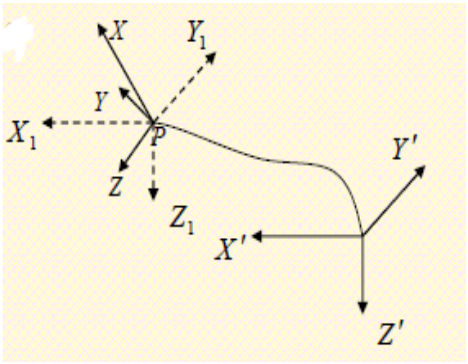

Figure 3-7 Frame Translation

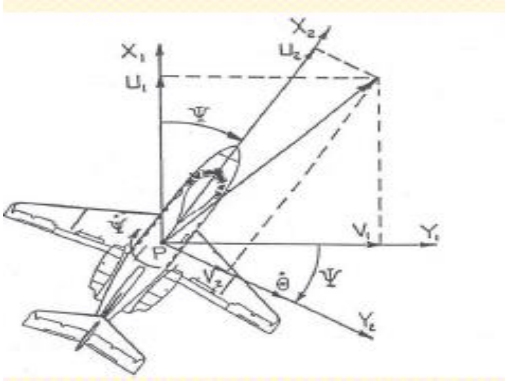

Figure 3-8 Rotation about Z_1 axis

•Common sequence:

$\boldsymbol{\psi, \theta, \phi}$

•Translate $\boldsymbol{X'Y'Z'}$ parallel to it until its center coincides with the $\boldsymbol{XYZ}$ system. Rename $\boldsymbol{X'Y'Z'}$ as $\boldsymbol{X_1Y_1Z_1}$ for convenience.

•Rotate the system $\boldsymbol{X_1Y_1Z_1}$ about $\boldsymbol{Z_1}$ axis over an angle $\boldsymbol{\psi}$. This yields the coordinate system $\boldsymbol{X_2Y_2Z_2}$.

- $[\boldsymbol{\phi} \quad \boldsymbol{\theta} \quad \boldsymbol{\psi}]^T$ = Euler Angles

- Rotate the system $\boldsymbol{X_2Y_2Z_2}$ about $\boldsymbol{Y_2}$ axis over an angle $\boldsymbol{\theta}$. This yields the coordinate system $\boldsymbol{X_3Y_3Z_3}$.

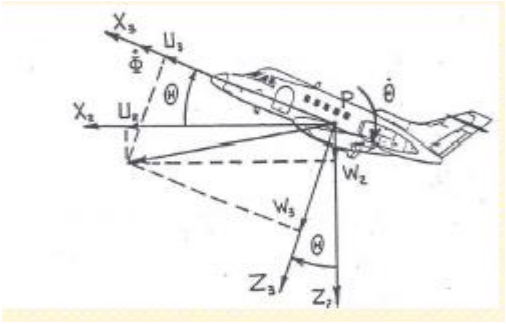

Figure 3-9 Rotation about Y_2 axis

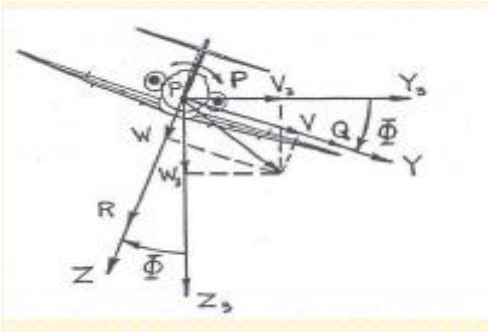

Figure 3-10 Rotation about X_3 axis

- Rotate the system $\boldsymbol{X_3Y_3Z_3}$ about $\boldsymbol{X_3}$ axis over an angle $\boldsymbol{\phi}$. This yields the coordinate system $\boldsymbol{XYZ}$.

- The transformation of each step is given below

$$\boldsymbol{X'Y'Z' \rightarrow X_1Y_1Z_1}$$

$$\begin{bmatrix} \dot{x}' \\ \dot{y}' \\ \dot{z}' \end{bmatrix} = \begin{bmatrix} U_1 \\ V_1 \\ W_1 \end{bmatrix} \rightarrow$$

$$\boldsymbol{X_1Y_1Z_1 \rightarrow X_2Y_2Z_2}$$

$$\begin{bmatrix} U_1 \\ V_1 \\ W_1 \end{bmatrix} = \begin{bmatrix} \cos\psi & -\sin\psi & 0 \\ \sin\psi & \cos\psi & 0 \\ 0 & 0 & 1 \end{bmatrix} \begin{bmatrix} U_2 \\ V_2 \\ W_2 \end{bmatrix}$$

$$\downarrow$$

$$\boldsymbol{Y_3Z_3 \rightarrow XYZ}$$

$$\begin{bmatrix} U_3 \\ V_3 \\ W_3 \end{bmatrix} = \begin{bmatrix} 1 & 0 & 0 \\ 0 & \cos\phi & -\sin\phi \\ 0 & \sin\phi & \cos\phi \end{bmatrix} \begin{bmatrix} U \\ V \\ W \end{bmatrix} \leftarrow$$

$$\boldsymbol{X_2Y_2Z_2 \rightarrow X_3Y_3Z_3}$$

$$\begin{bmatrix} U_2 \\ V_2 \\ W_2 \end{bmatrix} = \begin{bmatrix} \cos\theta & 0 & -\sin\theta \\ 0 & 1 & 0 \\ \sin\theta & 0 & \cos\theta \end{bmatrix} \begin{bmatrix} U_3 \\ V_3 \\ W_3 \end{bmatrix}$$

- So overall transformation from the inertial frame to body frame is given as follows:

$$\boldsymbol{X'Y'Z' \rightarrow XYZ}$$

$$\begin{bmatrix} U_1 \\ V_1 \\ W_1 \end{bmatrix} = \begin{bmatrix} \cos\psi & -\sin\psi & 0 \\ \sin\psi & \cos\psi & 0 \\ 0 & 0 & 1 \end{bmatrix} \begin{bmatrix} \cos\theta & 0 & -\sin\theta \\ 0 & 1 & 0 \\ \sin\theta & 0 & \cos\theta \end{bmatrix} \begin{bmatrix} 1 & 0 & 0 \\ 0 & \cos\phi & -\sin\phi \\ 0 & \sin\phi & \cos\phi \end{bmatrix} \begin{bmatrix} U \\ V \\ W \end{bmatrix}$$

- In our case transformation is from $\boldsymbol{F_G}$(gravity frame) to $\boldsymbol{F_p}$(fuselage frame). i.e. $\boldsymbol{F_G} = {}^{\boldsymbol{G}}\boldsymbol{R_p} * \boldsymbol{F_p}$

$${}^{G}R_p = \begin{bmatrix} \cos\psi & -\sin\psi & 0 \\ \sin\psi & \cos\psi & 0 \\ 0 & 0 & 1 \end{bmatrix} \begin{bmatrix} \cos\theta & 0 & -\sin\theta \\ 0 & 1 & 0 \\ \sin\theta & 0 & \cos\theta \end{bmatrix} \begin{bmatrix} 1 & 0 & 0 \\ 0 & \cos\phi & -\sin\phi \\ 0 & \sin\phi & \cos\phi \end{bmatrix} \quad (3\text{-}1)$$

- $O_G x_G y_G z_G$ is just a translated frame from ground frame of reference $O_g x_g y_g z_g$.
- $O_p x_p y_p z_p$ is rotated by Euler angle $[\boldsymbol{\phi} \quad \boldsymbol{\theta} \quad \boldsymbol{\psi}]^T$ from $O_G x_G y_G z_G$.
- O_p may not be the center of gravity of the fuselage.

3.3 VECTORS DESCRIBING THE AIRCRAFT MOTION

- Translation velocity $\boldsymbol{\mathcal{V}} = [U \quad V \quad W]^{\boldsymbol{T}}$
- Rotational vector $\boldsymbol{\omega} = [P \quad Q \quad R]^{\boldsymbol{T}}$
- Euler's angle written in vector form $\boldsymbol{\Phi} = [\phi \quad \theta \quad \psi]^{\boldsymbol{T}}$
- Translation of aircraft relative to ground $\boldsymbol{\mathcal{X}_g} = [x_g \quad y_g \quad z_g]^{\boldsymbol{T}}$
- State variables of the system $\mathbb{X} = [\boldsymbol{\mathcal{V}} \quad \boldsymbol{\omega} \quad \boldsymbol{\mathcal{X}_g} \quad \boldsymbol{\Phi}]^{\boldsymbol{T}}$
- Spatial vector $\boldsymbol{Y} = [\boldsymbol{\mathcal{V}} \quad \boldsymbol{\omega}]^{\boldsymbol{T}}$

$\boldsymbol{\Phi}$ and $\boldsymbol{\mathcal{X}_g}$ are obtained from the system kinematics. Whereas $\boldsymbol{\mathcal{V}}$ and $\boldsymbol{\omega}$ are obtained from the system dynamics. $\boldsymbol{\mathcal{V}}$ and $\boldsymbol{\omega}$ will be combinedly treated as spatial vector $\boldsymbol{Y_p}$ for ease of calculation and computing without so many assumptions.

3.4 SYSTEM KINEMATICS

Translational Kinematics

Considering the translational motion of the aircraft this is direct transformation changing linear velocities, $[U \quad V \quad W]^T$ from $\boldsymbol{F_p}$(fuselage frame) to $\boldsymbol{F_G}$(gravity frame).

$$\begin{bmatrix} \dot{x}_g \\ \dot{y}_g \\ \dot{z}_g \end{bmatrix} = {}^{G}\boldsymbol{R}_{p} \begin{bmatrix} U \\ V \\ W \end{bmatrix}. \tag{3-2}$$

Where ${}^{G}\boldsymbol{R}_{p}$ is the rotation matrix from fuselage frame to gravity frame with an Euler angle rotation of $[\phi \quad \theta \quad \psi]^T$ w.r.t. $[x_g \quad y_g \quad z_g]^T$ axes respectively.

Rotational Kinematics

For obtaining $[\phi \quad \theta \quad \psi]^T$ we have to find a relationship between $[\dot{\phi} \quad \dot{\theta} \quad \dot{\psi}]^T$ and $[P \quad Q \quad R]^T$ and then integrate it.

$$\vec{\boldsymbol{\omega}} = \hat{\imath}P + \hat{\jmath}Q + \hat{k}R = \dot{\vec{\phi}} + \dot{\vec{\theta}} + \dot{\vec{\psi}}$$

Using coordinate transformation rules we can find that

$$\begin{bmatrix} \dot{\phi} \\ \dot{\theta} \\ \dot{\psi} \end{bmatrix} = \begin{bmatrix} 1 & \sin\phi \tan\theta & \cos\phi \tan\theta \\ 0 & \cos\phi & -\sin\phi \\ 0 & \sin\phi \sec\theta & \cos\phi \sec\theta \end{bmatrix} \begin{bmatrix} P \\ Q \\ R \end{bmatrix} \tag{3-3}$$

3.5 SYSTEM DYNAMICS & EQUATIONS OF MOTION

The equations of motion of the aircraft are derived using d'Alembert's principle, summing up at point O_p all the loads (forces and moments) acting on the fuselage, wings, nacelles, empennage, and rotors. The system of six equations of motion is obtained which may be grouped as two subsystems for forces and moments acting on the fuselage and wings (index p), two nacelles and two rotors.

$$\mathbb{F}_{\boldsymbol{p}} + \mathbb{F}_{\boldsymbol{nl}} + \mathbb{F}_{\boldsymbol{nr}} + \mathbb{F}_{\boldsymbol{rl}} + \mathbb{F}_{\boldsymbol{rr}} = \mathbf{0} \quad \Rightarrow \text{Forces on the system} \tag{3-4}$$

$$\mathbb{M}_{\boldsymbol{p}} + \mathbb{M}_{\boldsymbol{nl}} + \mathbb{M}_{\boldsymbol{nr}} + \mathbb{M}_{\boldsymbol{rl}} + \mathbb{M}_{\boldsymbol{rr}} = \mathbf{0} \quad \Rightarrow \text{Moments on the system} \tag{3-5}$$

Each element of the above equation consists of inertia, aerodynamic and gravity loads.

$$\mathbf{Q}_{()} = [\mathbb{F}_{()} \quad \mathbb{M}_{()}]^{\boldsymbol{T}} = \mathbf{Q}_{()\boldsymbol{i}} + \mathbf{Q}_{()\boldsymbol{a}} + \mathbf{Q}_{()\boldsymbol{g}}$$

$\mathbf{Q}_{()\boldsymbol{i}}$ = Spatial vector of Inertia loads,

$\mathbf{Q}_{()\boldsymbol{a}}$ = Spatial vector Aerodynamic loads,

$\mathbf{Q}_{()\boldsymbol{g}}$ = Spatial vector Gravity spatial loads

Subscripts are defined as: **n(l/r)** for nacelle, **r(l/r)** for rotor, **p** for fuselage, **w** for wings, **HS** for horizontal stabilizers, **VS** for vertical stabilizers.

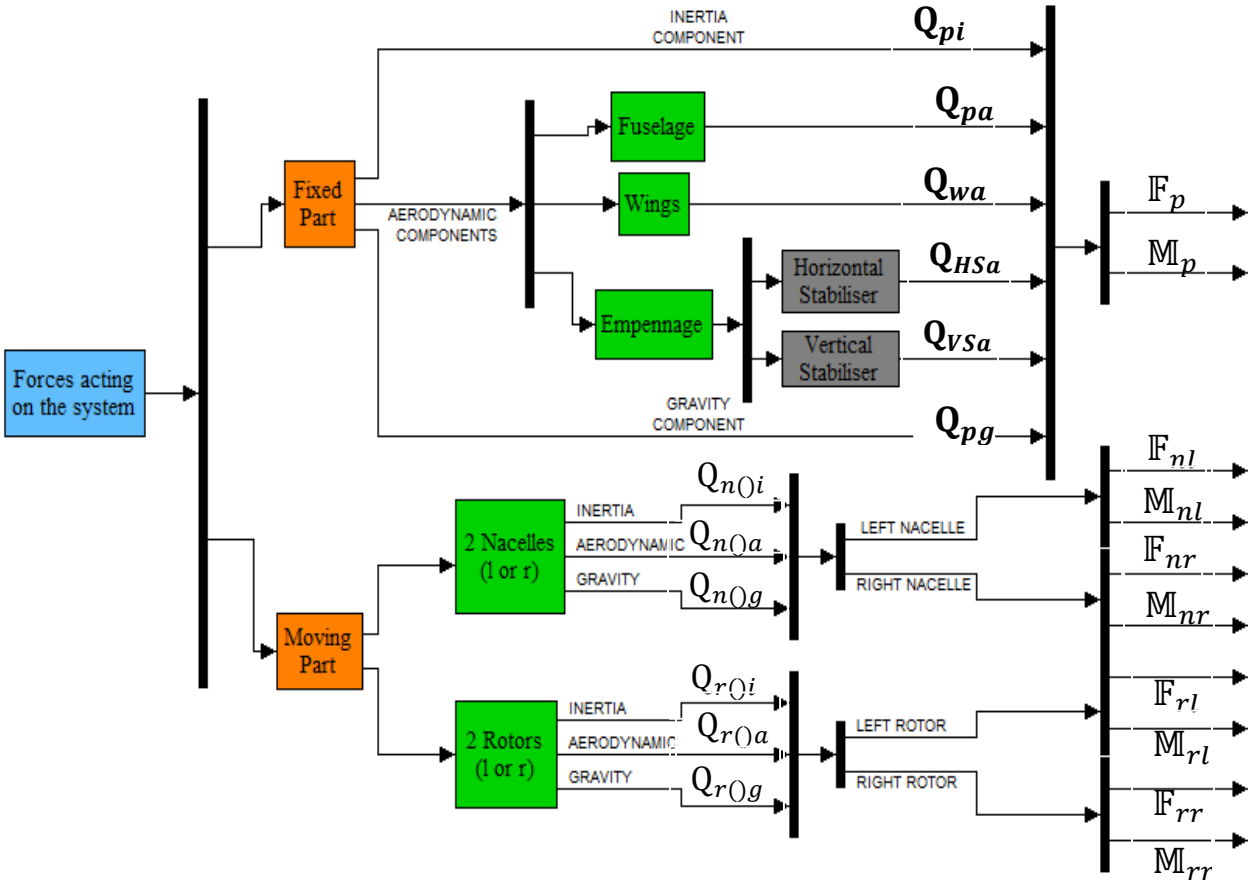

Figure 3-11 Forces Acting on the system

For calculation of all the above loads we need to consider about inertia tensor, rigid body dynamics, and aerodynamics of the body, which is given in the appendices. We can also solve for these loads by taking two subsystem i.e. one for rational dynamics and the other for translational dynamics, but by doing so the calculation will be very cumbersome unless we neglect centripetal and coriolis components due to non-inertial frame of reference.

Here we will analyze each kind of load one by one starting with inertia loads. Again each load is calculated separately for different parts of the aircraft separately. Again it is assumed that every part of the aircraft is rigid, i.e. there C.G. doesn't change with time w.r.t. their respective body-frame origins.

3.6 INERTIA LOADS

All the inertia loads are computed on the body frame of reference. This is obtained from the conservation of momentum. It is categorized into fixed part and moving part of the aircraft with respect to body-frame of fuselage.

Fixed Part Inertia Load

This consists of fuselage, wings, and empennage. And these three are considered as one entity for the inertia loads. From rigid body dynamics (Appendix B) it is obtained that

$$\mathbf{Q_{pi}} = \mathbb{I}_{\boldsymbol{p}}\dot{\boldsymbol{Y}}_{\boldsymbol{p}} + \boldsymbol{\Omega}_{\boldsymbol{p}}\mathbb{I}_{\boldsymbol{p}}\boldsymbol{Y}_{\boldsymbol{p}} \tag{3-6}$$

Whereas the spatial vector, $\boldsymbol{Y_p} = [U \quad V \quad W \quad P \quad Q \quad R]^{\boldsymbol{T}}$ is composed of components of aircraft translational velocities and rotational rates.

The inertia matrix, $\mathbb{I}_{\boldsymbol{p}}$ has the form

$$\mathbb{I}_{\boldsymbol{p}} = \begin{bmatrix} m_p & 0 & 0 & 0 & S_{zp} & -S_{yp} \\ 0 & m_p & 0 & -S_{zp} & 0 & S_{xp} \\ 0 & 0 & m_p & S_{yp} & -S_{xp} & 0 \\ 0 & -S_{zp} & S_{yp} & I_{xp} & -I_{xyp} & -I_{xzp} \\ S_{zp} & 0 & -S_{xp} & -I_{xyp} & I_{yp} & -I_{yzp} \\ -S_{yp} & S_{xp} & 0 & -I_{xzp} & -I_{yzp} & I_{zp} \end{bmatrix}, \quad \begin{aligned} S_{xp} &= m_p x_{pCG} \\ S_{yp} &= m_p y_{pCG} \\ S_{zp} &= m_p z_{pCG} \end{aligned}$$

$\overrightarrow{\boldsymbol{r_p}} = [x_{pCG} \quad y_{pCG} \quad z_{pCG}]^{\boldsymbol{T}}$, m_p = Mass of the fixed part of aircraft

Whereas $\left|\overrightarrow{\boldsymbol{r_p}}\right|$ is the distance between O_p (origin of fuselage coordinate system) and O_{pCG} (C.G. of the fixed part of aircraft).

Inertia tensor $\boldsymbol{I_p}$ at O_p is transformed from $\boldsymbol{I_{pCG}}$ at O_{pCG} as given bellow.

$$\boldsymbol{I_p = I_{pCG} - m_p S^2(r_p).}$$ (Described in Appendix A)

Whereas $\boldsymbol{S(r_p)}$ skewed matrix of the vector $\overrightarrow{\boldsymbol{r_p}}$**.** This is also described in Appendix A.

Velocity matrix $\boldsymbol{\Omega_p}$ is given as

$$\boldsymbol{\Omega_p} = \begin{bmatrix} 0 & -R & Q & 0 & 0 & 0 \\ R & 0 & -P & 0 & 0 & 0 \\ -Q & -P & 0 & 0 & 0 & 0 \\ 0 & -W_p & V_p & 0 & -R & Q \\ W_p & 0 & -U_p & R & 0 & -P \\ -V_p & U_p & 0 & -Q & P & 0 \end{bmatrix}, \text{ and } \begin{bmatrix} U_p \\ V_p \\ W_p \end{bmatrix} = \overrightarrow{\boldsymbol{r_p}} \times \overrightarrow{\boldsymbol{\omega_p}}$$

Moving Part Inertia Load

This consists of 2 nacelles and 2 rotors. The inertia components $\mathbf{Q_{nli}}, \mathbf{Q_{nri}}, \mathbf{Q_{rli}}, \mathbf{Q_{rri}}$ are computed relative to fuselage frame of reference. Subscript 'm' is for moving part.

$$\mathbf{Q_{mi}} = \mathbb{I}_{\boldsymbol{m}}\left(\dot{\boldsymbol{Y}}_{\boldsymbol{p}} + \dot{\boldsymbol{Y}}_{\boldsymbol{m}}\right) + \left(\boldsymbol{\Omega_p} + \boldsymbol{\Omega_m}\right)\mathbb{I}_{\boldsymbol{m}}\left(\boldsymbol{Y_p} + \boldsymbol{Y_m}\right)$$

3-7

For Nacelles:

Both nacelles are identical. The corresponding inertia and velocity matrix are as follows:

$$\mathbb{I}_{\boldsymbol{n}()} = \begin{bmatrix} m_n & 0 & 0 & 0 & S_{zn()} & -S_{yn()} \\ 0 & m_n & 0 & -S_{zn()} & 0 & S_{xn()} \\ 0 & 0 & m_n & S_{yn()} & -S_{xn()} & 0 \\ 0 & -S_{zn()} & S_{yn()} & I_{xn()} & -I_{xyn()} & -I_{xzn()} \\ S_{zn()} & 0 & -S_{xn()} & -I_{xn()} & I_{yn()} & -I_{yzn()} \\ -S_{yn()} & S_{xn()} & 0 & -I_{xzn()} & -I_{yzn()} & I_{zn()} \end{bmatrix}$$

( ) $\rightarrow$ can be 'l' or 'r'

Whereas $\begin{bmatrix} S_{xn()} \\ S_{yn()} \\ S_{zn()} \end{bmatrix} = m_n \overrightarrow{\boldsymbol{r'}_{\boldsymbol{n}()\boldsymbol{CG}}}$, and $\left|\overrightarrow{\boldsymbol{r'}_{\boldsymbol{n}()\boldsymbol{CG}}}\right|$ is the distance between $\boldsymbol{O_p}$ (origin of fuselage coordinate system) and $\boldsymbol{O_{n()CG}}$ (C.G of the corresponding nacelle).

$\overrightarrow{\boldsymbol{r}_{\boldsymbol{n}()\boldsymbol{CG}}}$ = vector representing $\boldsymbol{O_{n()CG}}$ in $O_{n()}x_{n()}y_{n()}z_{n()}$(nacelle reference frame $\boldsymbol{F_p}$)

$\overrightarrow{\boldsymbol{r}_{\boldsymbol{n}()}}$ = vector representing $O_{n()}$ in $O_p x_p y_p z_p$ (fuselage frame of reference $\boldsymbol{F_{n()}}$).

$$\overrightarrow{\boldsymbol{r'}_{\boldsymbol{n}()\boldsymbol{CG}}} = \overrightarrow{\boldsymbol{r}_{\boldsymbol{n}()}} + {}^{\boldsymbol{p}}\boldsymbol{R}_{\boldsymbol{n}()}\overrightarrow{\boldsymbol{r}_{\boldsymbol{n}()\boldsymbol{CG}}}$$

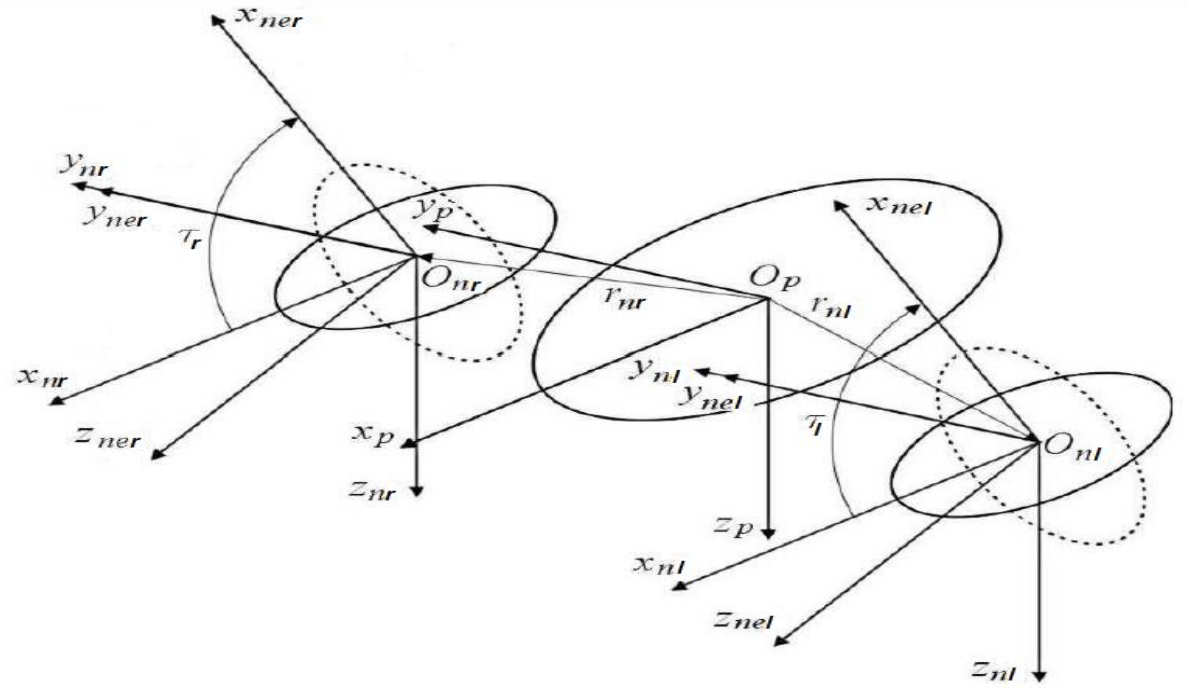

Figure 3-12 Nacelle Frame w.r.t. fuselage Frame

The spatial vector of nacelle w.r.t. $\boldsymbol{F_p}$ is $\boldsymbol{Y_{n()}} = [0 \quad 0 \quad 0 \quad 0 \quad \dot{\tau}_{()} \quad 0]^{\boldsymbol{T}}$, because the nacelle has only one degree of freedom w.r.t. fuselage i.e. tilting by an angle $\boldsymbol{\tau}$ about $y_{n()}$.

$$^{\boldsymbol{p}}\boldsymbol{R_{n()}} = \begin{bmatrix} \cos\tau_{()} & 0 & \sin\tau_{()} \\ 0 & 1 & 0 \\ -\sin\tau_{()} & 0 & \cos\tau_{()} \end{bmatrix}$$

Inertia tensor $\boldsymbol{I_{n()}}$ about $\boldsymbol{F_p}$ is obtained by transforming from $\boldsymbol{I_{n()CG}}$ (Inertia tensor about C.G. of corresponding nacelle).

$$\boldsymbol{I_{n()}} = {}^{\boldsymbol{p}}\boldsymbol{R}_{\boldsymbol{n()}}\boldsymbol{I_{n()CG}}\left({}^{\boldsymbol{p}}\boldsymbol{R}_{\boldsymbol{n()}}\right)^{\boldsymbol{T}} + \boldsymbol{I_{tn()}} \qquad \text{(Described in Appendix A)}$$

$\boldsymbol{I_{tn()}}$= Translation Matrix = $m_n\boldsymbol{S^2}\left(\boldsymbol{r'_{n()CG}}\right)$

The velocity matrix of the nacelle w.r.t fuselage $\boldsymbol{\Omega_{n()}}$ is given as

$$\boldsymbol{\Omega_{n()}} = \begin{bmatrix} 0 & 0 & \dot{\tau}_{()} & 0 & 0 & 0 \\ 0 & 0 & 0 & 0 & 0 & 0 \\ -\dot{\tau}_{()} & 0 & 0 & 0 & 0 & 0 \\ 0 & -W_{n()} & V_{n()} & 0 & 0 & \dot{\tau}_{()} \\ W_{n()} & 0 & -U_{n()} & 0 & 0 & 0 \\ -V_{n()} & U_{n()} & 0 & -\dot{\tau}_{()} & 0 & 0 \end{bmatrix}, \begin{bmatrix} U_{n()} \\ V_{n()} \\ W_{n()} \end{bmatrix} = \overrightarrow{\boldsymbol{r'}_{\text{n()CG}}} \times \begin{bmatrix} 0 \\ \dot{\tau}_{()} \\ 0 \end{bmatrix}$$

For Rotors:

Both rotors are identical. The C.G. of the rotor and $O_{h()}$ are the same corresponding inertia and velocity matrix are as follows:

$$\mathbb{I}_{\boldsymbol{n()}} = \begin{bmatrix} m_r\mathbf{I}_{3\text{x}3} & -m_r\boldsymbol{S}\left(\boldsymbol{r'}_{\boldsymbol{r()}}\right) \\ m_r\boldsymbol{S}\left(\boldsymbol{r'}_{\boldsymbol{r()}}\right) & \boldsymbol{I}_{\text{r()}} \end{bmatrix}, \quad \mathbf{I}_{3\text{x}3} = \text{Identity matrix}, \quad \boldsymbol{I}_{\text{r()}} = \text{Inertia matrix of rotor w. r. t. } \boldsymbol{F_p}$$

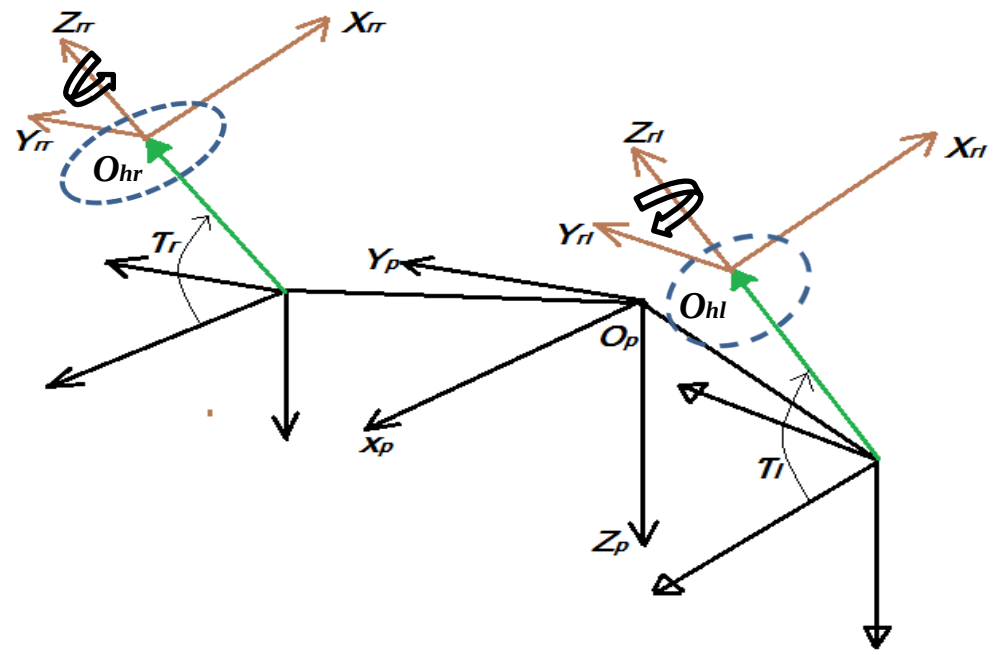

Figure 3-13 Hub reference frame w.r.t. fuselage

$\overrightarrow{r'_{r0}}$ = Vector representing the hub center (C.G. of rotor) from O_p.

$\overrightarrow{r_{r0}} = [l \quad 0 \quad 0]^T$ = Vector representing the hub center from O_{n0}.

$$\overrightarrow{r'_{r0}} = \overrightarrow{r_{n0}} + {}^{p}R_{n0}\overrightarrow{r_{r0}}$$

Velocity of the hub center w.r.t. O_p will be:

$$\overrightarrow{v_{r0}} = \frac{d\overrightarrow{r'_{r0}}}{dt} = \frac{d\overrightarrow{r_{n0}}}{dt} + \frac{d\,{}^{p}R_{n0}}{dt} + \frac{d\overrightarrow{r_{r0}}}{dt}$$

$$\Rightarrow \overrightarrow{v_{r0}} = \frac{d\,{}^{p}R_{n0}}{dt} \qquad (\because \overrightarrow{r_{n0}}, \overrightarrow{r_{r0}} \text{ Doesn't vary with time})$$

$$\Rightarrow \overrightarrow{v_{r0}} = \begin{bmatrix} -\dot{\tau_0}\sin\tau_0 & 0 & \dot{\tau_0}\cos\tau_0 \\ 0 & 1 & 0 \\ -\dot{\tau_0}\cos\tau_0 & 0 & -\dot{\tau_0}\sin\tau_0 \end{bmatrix} \begin{bmatrix} l \\ 0 \\ 0 \end{bmatrix}$$

$$\Rightarrow \overrightarrow{\boldsymbol{v}_{r()}} = \begin{bmatrix} -l\,\dot{\tau}_{()}\sin\tau_{()} \\ 0 \\ -l\,\dot{\tau}_{()}\cos\tau_{()} \end{bmatrix}$$

Rotational rates of the hub center w.r.t. $\boldsymbol{O_p}$ will be:

$\overrightarrow{\boldsymbol{\omega'}_{r()}} = {}^{p}\boldsymbol{R}_{r()}\overrightarrow{\boldsymbol{\omega}_{r()}}$, $\omega_{r()}$= angular speed of the rotor

$$\overrightarrow{\boldsymbol{\omega'}_{r()}} = \begin{bmatrix} \cos(\tau_{()}+90°) & 0 & \sin(\tau_{()}+90°) \\ 0 & 1 & 0 \\ -\sin(\tau_{()}+90°) & 0 & \cos(\tau_{()}+90°) \end{bmatrix}\begin{bmatrix} 0 \\ 0 \\ \omega_{r()} \end{bmatrix}$$

$$\overrightarrow{\boldsymbol{\omega'}_{r()}} = \begin{bmatrix} \omega_{r()}\cos\tau_{()} \\ 0 \\ -\omega_{r()}\sin\tau_{()} \end{bmatrix}$$

So the spatial vector of rotor w.r.t. fuselage $\boldsymbol{Y_{r()}} = [\boldsymbol{v_{r()}} \quad \boldsymbol{\omega'}_{r()}]^{\boldsymbol{T}}$

Rotor inertia tensor w.r.t rotor = $\boldsymbol{I}_{\mathrm{r}()\boldsymbol{CG}}$

Rotor inertia tensor w.r.t. $\boldsymbol{F_p}$= $\boldsymbol{I}_{\mathrm{r}()}$

$$\boldsymbol{I}_{\mathrm{r}()} = {}^{p}\boldsymbol{R}_{r()}\boldsymbol{I}_{\mathrm{r}()\boldsymbol{CG}}\left({}^{p}\boldsymbol{R}_{r()}\right)^{\boldsymbol{T}} + \boldsymbol{m_r S^2}\left(\boldsymbol{r'}_{r()}\right) \tag{3-8}$$

Till now only the inertia loads are calculated i.e.at the center of fuselage coordinate system. Next the Gravity loads are to be calculated.

3.7 GRAVITY LOADS

The gravity forces and moments are calculated 1st in the center of gravity of each part of the aircraft. Next they are transformed to the center $\boldsymbol{O_p}$ of the fuselage system of coordinate.

The vector of gravity acceleration in the gravity system of coordinates has the form $\overrightarrow{\boldsymbol{g}_G} = [0 \quad 0 \quad g]^T$.

Fixed Part Gravity Load

In the fixed part the masses of the fuselage, wings, and empennage are accounted for together and the gravity loads of these parts are calculated as fuselage gravity loads.

1st the gravity vector is obtained w.r.t. the fuselage system of coordinates using the following transformation:

$$\overrightarrow{\boldsymbol{g}_p} = {}^{\boldsymbol{P}}\boldsymbol{R}_{\boldsymbol{G}}\overrightarrow{\boldsymbol{g}_G}$$

Gravity force on fuselage coordinate system: $\mathbb{F}_{\boldsymbol{pg}} = m_p\overrightarrow{\boldsymbol{g}_p} = m_p\,{}^{\boldsymbol{P}}\boldsymbol{R}_{\boldsymbol{G}}\overrightarrow{\boldsymbol{g}_G}$

Gravity moment on fuselage frame: $\mathbb{M}_{\boldsymbol{pg}} = \overrightarrow{\boldsymbol{r}_p} \times \mathbb{F}_{\boldsymbol{pg}} = \overrightarrow{\boldsymbol{r}_p} \times \left(m_p\,{}^{\boldsymbol{P}}\boldsymbol{R}_{\boldsymbol{G}}\overrightarrow{\boldsymbol{g}_G}\right)$

$$= \boldsymbol{S}(\boldsymbol{r}_p) \times \left(m_p\,{}^{\boldsymbol{P}}\boldsymbol{R}_{\boldsymbol{G}}\overrightarrow{\boldsymbol{g}_G}\right)$$

So $\mathbf{Q}_{\boldsymbol{pg}} = \begin{bmatrix}\mathbb{F}_{\boldsymbol{pg}} \\ \mathbb{M}_{\boldsymbol{pg}}\end{bmatrix}$

3-9

Moving Part Gravity Load

The position of C.G. of moving parts of the local coordinates is calculated as $\overrightarrow{\boldsymbol{r'}_{()\boldsymbol{CG}}} = \overrightarrow{\boldsymbol{r}_{()}} + {}^{\boldsymbol{p}}\boldsymbol{R}_{()}\overrightarrow{\boldsymbol{r}_{()\boldsymbol{CG}}}$. Where $\overrightarrow{\boldsymbol{r'}_{()\boldsymbol{CG}}}$ id the vector of C.G. of the given element relative to the fuselage center. ${}^{\boldsymbol{p}}\boldsymbol{R}_{()}$ is the general description of the matrix of the rotation of the local system of coordinate (fixed to the element) relative to the fuselage system of coordinate. $\overrightarrow{\boldsymbol{r}_{()\boldsymbol{CG}}}$ is the vector of position of C.G. of the element in the local coordinate system. So the gravity load of the moving elements can be calculated as follows:

Nacelles (left /Right) Gravity Load

Gravity force acting on the nacelle in $\boldsymbol{F_p}$: $\mathbb{F}_{\boldsymbol{n()g}} = m_n\overrightarrow{\boldsymbol{g}_p} = m_n\,{}^{\boldsymbol{P}}\boldsymbol{R}_{\boldsymbol{G}}\overrightarrow{\boldsymbol{g}_G}$

Gravity moment on nacelle in $\boldsymbol{F_p}$: $\mathbb{M}_{\boldsymbol{n()g}} = \overrightarrow{\boldsymbol{r'}_{\boldsymbol{n()CG}}} \times \mathbb{F}_{\boldsymbol{n()g}}$

$$= \boldsymbol{S}\left(\boldsymbol{r'}_{\boldsymbol{n()CG}}\right) \times \left(m_n\,{}^{\boldsymbol{P}}\boldsymbol{R}_{\boldsymbol{G}}\overrightarrow{\boldsymbol{g}_G}\right)$$

So $\mathbf{Q}_{\boldsymbol{n}()\boldsymbol{g}} = \begin{bmatrix} \mathbb{F}_{\boldsymbol{n}()\boldsymbol{g}} \\ \mathbb{M}_{\boldsymbol{n}()\boldsymbol{g}} \end{bmatrix}$ (3-10)

Rotors (left/right) Gravity load

Gravity force acting on the rotor in $\boldsymbol{F_p}$: $\mathbb{F}_{\boldsymbol{r}()\boldsymbol{g}} = m_r \overrightarrow{\boldsymbol{g}_p} = m_r \, {}^{\boldsymbol{P}}\boldsymbol{R}_{\boldsymbol{G}} \overrightarrow{\boldsymbol{g}_G}$

$\overrightarrow{\boldsymbol{r'}_{\boldsymbol{r}()\boldsymbol{CG}}} = \overrightarrow{\boldsymbol{r'}_{\boldsymbol{r}()}}$ (∵ The hub center is the C.G. of rotor)

Gravity moment on nacelle in $\boldsymbol{F_p}$: $\mathbb{M}_{\boldsymbol{r}()\boldsymbol{g}} = \overrightarrow{\boldsymbol{r'}_{\boldsymbol{r}()\boldsymbol{CG}}} \times \mathbb{F}_{\boldsymbol{r}()\boldsymbol{g}}$

$= \boldsymbol{S}\left(\boldsymbol{r'}_{\boldsymbol{r}()\boldsymbol{CG}}\right) \times \left(m_r \, {}^{\boldsymbol{P}}\boldsymbol{R}_{\boldsymbol{G}} \overrightarrow{\boldsymbol{g}_G}\right)$

So $\mathbf{Q}_{\boldsymbol{r}()\boldsymbol{g}} = \begin{bmatrix} \mathbb{F}_{\boldsymbol{r}()\boldsymbol{g}} \\ \mathbb{M}_{\boldsymbol{r}()\boldsymbol{g}} \end{bmatrix}$

3-11

3.8 AERODYNAMIC LOADS

Aerodynamic loads can be calculated part wise individually viz. fuselage, empennage, horizontal stabilizer, vertical stabilizer, nacelle and then rotor.

But the modern day Computational Fluid Dynamics (CFD) software can easily give the forces acting on a fixed entity at a given operating condition. The input to the software is the 3D CAD model of the structure. And as the flight range will be local the air density is assumed to be constant for a particular flight run.

After all the considerations we only have to find the aerodynamic loads of the following parts:-

1) Fixed part (Consists of fuselage, wings & empennage)
2) Moving Parts
    a. Nacelle (Left and Right)

b. Rotor (Left and Right)

Computation of aerodynamic forces on the fixed part and nacelle is done by CFD based software. The same for the rotors is done by considering the classical 'Momentum Theory' and the 'Blade Element Theory' for simpler calculation.

Fixed Part Aerodynamic Loads

Directly the forces and moments are found about the body frame by the CFD analysis of the 3D structure of the aircraft at a particular value of air density and low mach number. And the forces and moments are dependent on the angle of incidence ($\boldsymbol{\alpha}$), angle of side slip ($\boldsymbol{\beta}$), the relative velocity $\left|\overrightarrow{\mathbb{V}_r}\right|$. $\mathbb{V}_r$ is the vectorial difference between aircraft's velocity and the wind velocity in the body frame of reference.

Let $\left|\overrightarrow{\mathbb{V}_w}\right|$ is the wind velocity in defined in the gravity frame of reference.

Then $\overrightarrow{\mathbb{V}_r} = \overrightarrow{\mathbb{V}_P} - {}^{P}\boldsymbol{R}_{G}\overrightarrow{\mathbb{V}_w}$. $\overrightarrow{\mathbb{V}_P}$ is the aircraft velocity in body frame. ${}^{P}\boldsymbol{R}_{G}$ is the rotation matrix from gravity frame to body frame.

$\boldsymbol{\alpha_P} = \frac{-W_r}{\sqrt{{U_r}^2+{V_r}^2+{W_r}^2}} = \frac{-W_r}{|\overrightarrow{\mathbb{V}_r}|}$ = angle of incidence.

$\boldsymbol{\beta_P} = \frac{V_r}{\sqrt{{U_r}^2+{V_r}^2}}$ = angle of sideslip

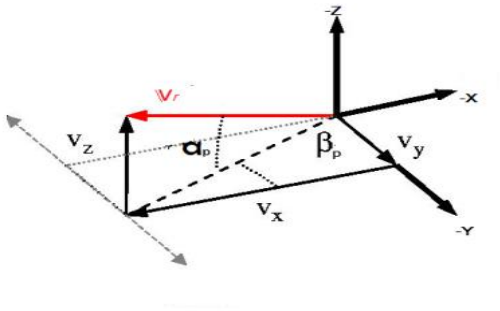

Figure 3-14 Angle of Incidence and side slip

So the aerodynamic forces and moments are:

$$\begin{bmatrix}\mathbb{F}_{Pa}\\ \mathbb{M}_{Pa}\end{bmatrix} = \begin{bmatrix} F_{xPa}(\boldsymbol{\alpha_P},\boldsymbol{\beta_P},\left|\overrightarrow{\mathbb{V}_r}\right|)\\ F_{yPa}(\boldsymbol{\alpha_P},\boldsymbol{\beta_P},\left|\overrightarrow{\mathbb{V}_r}\right|)\\ F_{zPa}(\boldsymbol{\alpha_P},\boldsymbol{\beta_P},\left|\overrightarrow{\mathbb{V}_r}\right|)\\ M_{xPa}(\boldsymbol{\alpha_P},\boldsymbol{\beta_P},\left|\overrightarrow{\mathbb{V}_r}\right|)\\ M_{yPa}(\boldsymbol{\alpha_P},\boldsymbol{\beta_P},\left|\overrightarrow{\mathbb{V}_r}\right|)\\ M_{zPa}(\boldsymbol{\alpha_P},\boldsymbol{\beta_P},\left|\overrightarrow{\mathbb{V}_r}\right|) \end{bmatrix}$$

. Each element in this vector is a function of $\boldsymbol{\alpha_P},\boldsymbol{\beta_P},\left|\overrightarrow{\mathbb{V}_r}\right|$

This 6 dimensional vector is found out by look up table method, which has 3 inputs, and the data are interpolated to get an approximate value which is very close to the actual value.

Moving Part Aerodynamic Loads

For Nacelle (left / right):

Here the forces are calculated in the moving reference frames then it is transferred to the body reference frame.

The relative velocity in the nacelle and the wind in the nacelle frame of reference is given by: $\overrightarrow{\mathbb{V}_r^{n()}} = {}^{n()}\boldsymbol{R}_{\boldsymbol{P}}\overrightarrow{\mathbb{V}_P} - {}^{n()}\boldsymbol{R}_{\boldsymbol{P}}{}^{\boldsymbol{P}}\boldsymbol{R}_{\boldsymbol{G}}\overrightarrow{\mathbb{V}_w} = {}^{n()}\boldsymbol{R}_{\boldsymbol{P}}\overrightarrow{\mathbb{V}_r} = \begin{bmatrix} U_r\cos\tau_{()} - W_r\sin\tau_{()} \\ V_r \\ U_r\sin\tau_{()} + W_r\cos\tau_{()} \end{bmatrix}$

And $\left|\overrightarrow{\mathbb{V}_r^{n()}}\right| = \left|\overrightarrow{\mathbb{V}_r}\right|$, i.e. the vectors represent same vector in different reference frames.

The angle of incidence and the angle of side slip for this case is given by:

$\boldsymbol{\alpha_{n()}} = \frac{-(U_r\sin\tau_{()} + W_r\cos\tau_{()})}{\left|\overrightarrow{\mathbb{V}_r}\right|}$ = Angle of incidence

$\boldsymbol{\beta_P} = \frac{\boldsymbol{V_r}}{\sqrt{\left(U_r\cos\tau_{()} - W_r\sin\tau_{()}\right)^2 + \boldsymbol{V_r}^2}}$ = Angle of sideslip

So the forces and moments about nacelle frames are given as below:

$$\begin{bmatrix} \mathbb{F}_{\boldsymbol{n()a}}^{\boldsymbol{n()}} \\ \mathbb{M}_{\boldsymbol{n()a}}^{\boldsymbol{n()}} \end{bmatrix} = \begin{bmatrix} F_{xn()a}(\boldsymbol{\alpha_{n()}}, \boldsymbol{\beta_{n()}}, \left|\overrightarrow{\mathbb{V}_r}\right|) \\ F_{yn()a}(\boldsymbol{\alpha_{n()}}, \boldsymbol{\beta_{n()}}, \left|\overrightarrow{\mathbb{V}_r}\right|) \\ F_{zn()a}(\boldsymbol{\alpha_{n()}}, \boldsymbol{\beta_{n()}}, \left|\overrightarrow{\mathbb{V}_r}\right|) \\ M_{xn()a}(\boldsymbol{\alpha_{n()}}, \boldsymbol{\beta_{n()}}, \left|\overrightarrow{\mathbb{V}_r}\right|) \\ M_{yn()Pa}(\boldsymbol{\alpha_{n()}}, \boldsymbol{\beta_{n()}}, \left|\overrightarrow{\mathbb{V}_r}\right|) \\ M_{zn()a}(\boldsymbol{\alpha_{n()}}, \boldsymbol{\beta_{n()}}, \left|\overrightarrow{\mathbb{V}_r}\right|) \end{bmatrix}$$

The above 6 dimensional vector is also obtained from the look up table procedure with 3 inputs to the look up table.

Now the transformation of this vector to the body frame reference is given by:

$$\overrightarrow{\mathbb{F}^{P}_{n()a}} = {}^{P}\boldsymbol{R}_{n()}\overrightarrow{\mathbb{F}^{n()}_{n()a}} \text{ (Force transformation)} \quad (3\text{-}12)$$

$$\overrightarrow{\mathbb{M}^{P}_{n()a}} = {}^{P}\boldsymbol{R}_{n()}\overrightarrow{\mathbb{M}^{n()}_{n()a}} + \begin{bmatrix}\mathbf{0}\\ \pm\boldsymbol{l}\\ \mathbf{0}\end{bmatrix} \times {}^{P}\boldsymbol{R}_{n()}\overrightarrow{\mathbb{F}^{n()}_{n()a}} \quad \mathbf{3\text{-}13}$$

Where l is the distance between body frame centers to the center of nacelle frame.

'+' sign is for right nacelle and '−' sign is for left nacelle.

So ultimately the transformation is given by:

$$\begin{bmatrix}\overrightarrow{\mathbb{F}^{P}_{n()a}}\\ \overrightarrow{\mathbb{M}^{P}_{n()a}}\end{bmatrix} = \begin{bmatrix}{}^{P}\boldsymbol{R}_{n()} & \mathbf{0}_{3\times3}\\ \mathbf{Skew}\left(\begin{bmatrix}\mathbf{0}\\ \pm\boldsymbol{l}\\ \mathbf{0}\end{bmatrix}\right) & {}^{P}\boldsymbol{R}_{n()}\end{bmatrix}\begin{bmatrix}\overrightarrow{\mathbb{F}^{n()}_{n()a}}\\ \overrightarrow{\mathbb{M}^{n()}_{n()a}}\end{bmatrix} \quad (3\text{-}14)$$

For Rotor:

Momentum Theory:

This theory uses the conservation laws of mass, momentum and energy. The rotor is considered as an actuator disk and is permeable to the air flow, but it supplies a pressure difference.

In this theory details of blade operating conditions are not considered. Uniform inflow is assumed. So that minimum induced power loss occurs.$\boldsymbol{v}$ is the normal inflow velocity to the rotor disk. The Power to lift the weight is called induced power.

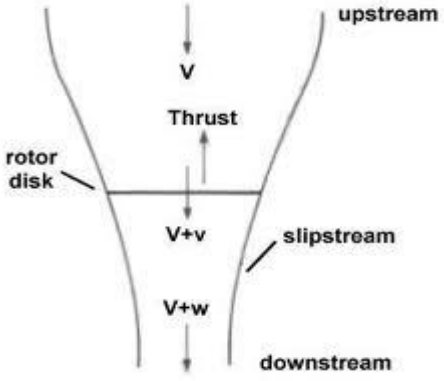

Figure 3-15 Momentum Theory

Rotor disk area$= \pi R^2 = A$

The mass flow rate at the rotor disk $= \dot{\boldsymbol{m}} = \boldsymbol{\rho A v}$ **3-15**

The thrust T is the change in momentum from far field upstream to far field downstream.

$$\mathbf{T} = \dot{m}w = \rho A v w \tag{3-16}$$

Energy conservation $\mathbf{T}v = \frac{1}{2}\dot{m}w^2 = \frac{1}{2}\rho A v w^2$

So, $w = 2v$, and $\mathbf{T} = 2\rho A v^2$ (3-17)

Blade Element Theory

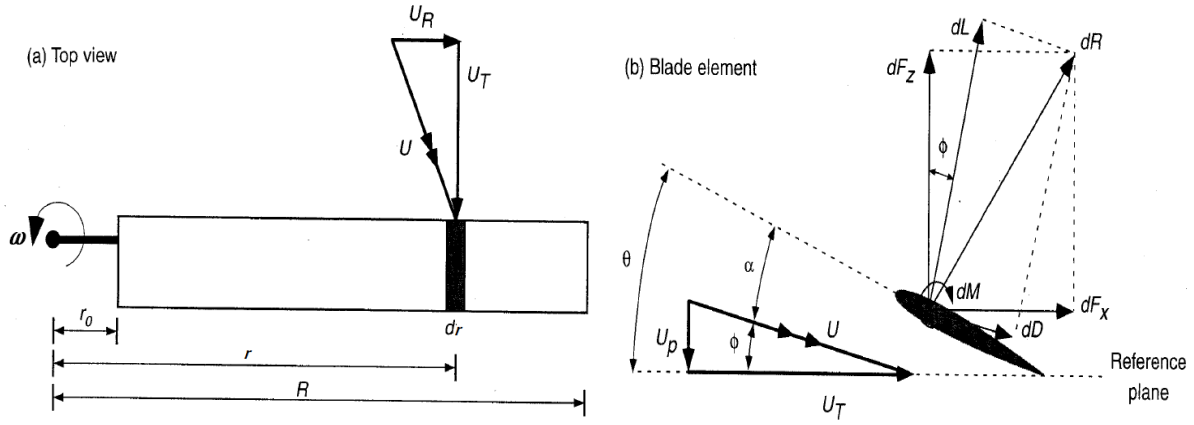

Figure 3-16 Blade Element Theory

$\boldsymbol{\theta}$ is the pitch of the blade w.r.t the rotor disk plane.

$\boldsymbol{\alpha}$ is the angle of attack.

And $= \tan^{-1}\frac{U_P}{U_T}$, where $\boldsymbol{U_P}$ is the perpendicular inflow to the blade and $\boldsymbol{U_T}$ is the horizontal one.

$\boldsymbol{U_T = \omega r}$ and $\boldsymbol{U_P = v + V_c}$. Where V_c is the climb velocity.

In this case climb velocity is nothing but $[0 \quad 0 \quad 1]^{r()}\boldsymbol{R_P}\overrightarrow{\mathbb{V}_r}$, i.e. the 'z' component of relative velocity in rotor frame of reference.

$\boldsymbol{\phi} \approx \frac{U_P}{U_T}$, as $\boldsymbol{U_T \gg U_P}$

For an airfoil of width $\boldsymbol{dr}$ the lift is $\boldsymbol{L = \frac{1}{2}\rho V_{in}{}^2 c C_{l\alpha} dr}$ (3-18)

$\boldsymbol{c}$ =Cord length

$\boldsymbol{V_{in}}$=inflow velocity $\approx \boldsymbol{\omega r}$

$\boldsymbol{C_{l\alpha}}$= Lift co-efficient at a particular $\boldsymbol{\alpha}$.

As we think of small angles of attack $\boldsymbol{C_{l\alpha}}$ can be approximated to $a_0\boldsymbol{\alpha} + a_1$

$$\boldsymbol{\alpha} = \boldsymbol{\theta} - \frac{\boldsymbol{U_P}}{\boldsymbol{U_T}}$$

So the total thrust is $\mathrm{T} = 3 * \int_0^R \frac{1}{2}\rho {V_{in}}^2 c C_{l\alpha} dr$

$$= 3 * \int_0^R \frac{1}{2}\rho {V_{in}}^2 c(a_0\alpha + a_1)dr$$

$$\mathbf{T} = \mathbf{3} * \int_{\mathbf{0}}^{\boldsymbol{R}} \frac{\mathbf{1}}{\mathbf{2}}\boldsymbol{\rho}{\boldsymbol{V_{in}}}^{\mathbf{2}}\boldsymbol{c}\left(\boldsymbol{a_0}\left(\boldsymbol{\theta} - \frac{\boldsymbol{U_P}}{\boldsymbol{U_T}}\right) + \boldsymbol{a_1}\right)\boldsymbol{dr}$$

3-19

From equation 5-16, and equation 5-14 it is found that

$$\mathbf{T} + \mathbf{K_1}\boldsymbol{\omega}\sqrt{\mathbf{T}} = \mathbf{K_2}\boldsymbol{\omega}^{\mathbf{2}} - \mathbf{K_3}\boldsymbol{\omega}[0 \quad 0 \quad 1]^{\boldsymbol{r}()}\boldsymbol{R_P}\overrightarrow{\mathbb{V}_r} \tag{3-20}$$

Where K_1, K_2 and K_3 are constants based on the rotor geometry air density. Here T is nothing but the force on the 'z' direction of the rotor.

So $\begin{bmatrix} \mathbb{F}_{\boldsymbol{r}()\boldsymbol{a}}^{\boldsymbol{r}()} \\ \mathbb{M}_{\boldsymbol{r}()\boldsymbol{a}}^{\boldsymbol{r}()} \end{bmatrix} = \begin{bmatrix} 0 \\ \mathrm{T}_{()} \\ 0 \\ 0 \\ 0 \\ 0 \end{bmatrix}$, Moment at the rotor frame is considered zero because the motor torque and drag torque are almost same and the residual torque is canceled by the counter rotating rotor pair, i.e. left rotor and right rotor.

Now if we transform this to the body frame reference:

$\overrightarrow{\mathbb{F}_{r()a}^{P}} = {}^{P}R_{r()}\overrightarrow{\mathbb{F}_{r()a}^{r()}}$ (Force transformation)

$\overrightarrow{\mathbb{M}_{\boldsymbol{r}()\boldsymbol{a}}^{\boldsymbol{P}}} = \overrightarrow{\boldsymbol{r'}_{\boldsymbol{r}()}} \times {}^{P}R_{n()}\overrightarrow{\mathbb{F}_{r()a}^{r()}}$

So the forces and moments at the body frame:

$$\begin{bmatrix} \overrightarrow{\mathbb{F}_{\boldsymbol{r}()\boldsymbol{a}}^{\boldsymbol{P}}} \\ \overrightarrow{\mathbb{M}_{\boldsymbol{r}()\boldsymbol{a}}^{\boldsymbol{P}}} \end{bmatrix} = \begin{bmatrix} {}^{\boldsymbol{P}}\boldsymbol{R}_{\boldsymbol{r}()} & \mathbf{0}_{3\times3} \\ \mathbf{Skew}(\overrightarrow{\boldsymbol{r'}_{\boldsymbol{r}()}}) & {}^{\boldsymbol{P}}\boldsymbol{R}_{\boldsymbol{r}()} \end{bmatrix} \begin{bmatrix} \overrightarrow{\mathbb{F}_{\boldsymbol{r}()\boldsymbol{a}}^{\boldsymbol{r}()}} \\ \overrightarrow{\mathbb{M}_{\boldsymbol{r}()\boldsymbol{a}}^{\boldsymbol{r}()}} \end{bmatrix} \tag{3-21}$$

Total aerodynamic load $\mathbf{Q_a} = \mathbf{Q_{Pa}} + \sum_{l,r}\mathbf{Q_{n()a}} + \sum_{l,r}\mathbf{Q_{r()a}}$ (3-22)

Equation of Motion

As we know inertia load is the nothing but the sum of the gravity load and aerodynamic loads

$$\mathbf{Q}_i = \mathbf{Q}_g + \mathbf{Q}_a \tag{3-23}$$

From the above mathematical modeling we came to know that our state variables are:

$$[U \quad V \quad W \quad P \quad Q \quad R \quad \phi \quad \theta \quad \psi \quad x_g \quad y_g \quad z_g \,]^T$$

And the control variables are: $[\omega_l \quad \omega_r \quad \tau_l \quad \tau_r]^T$

From the above model it is clear it is a non-linear system and non-affine control inputs also. So to control this and for tracking purposes we need to have non-linear, non-affine control techniques.

Chapter 4
Control Design

For the control design we need to know the state variables. After that we need to find a control function $\boldsymbol{u}$ which is a 4 dimensional vector as stated in chapter 3(the control variables).

For the nonlinearity of the system and satisfying the tracking of desired response the state feedback linearization or the Dynamic Inversion technique is use. Again as the system is nonaffine-in-control the Dynamic Inversion is used via time-scale separation. This is useful for a class of multivariable nonaffine-in-control systems via time-scale separation. The control signal is defined as a solution of "fast" dynamics, and the coupled system is shown to comply with the assumptions of Tikhonov's theorem from singular perturbations theory [16].

The basic design idea in relies on time-scale separation between the system and the controller dynamics [17]. The latter is designed to approximate the unknown dynamic inversion based control solution, assuming that it exists. For example, for a single-input system like

$\dot{x} = f(x,u), x(0) = x_0, t \geq 0$, where $x \in \mathbb{R}$ is the system state, $u \in \mathbb{R}$ is the control input, fast dynamics are introduced as follows: $\epsilon\dot{u} = -sign\left(\frac{\partial f}{\partial u}\right)(f(x,u) + ax)$, $a > 0, \epsilon \gg 1$. Assuming that f is a Lipschitz function of its arguments, and that $\frac{\partial f}{\partial u}$ is bounded away from zero for$(x,u) \in \Omega_x \times \Omega_y \subset R \times R$, where Ω_x , $\Omega_y$are compact sets, as per the singular perturbation theorem. This theorem can be shown extended for the multi-input systems as well, and can be shown that the use of $sign\left(\frac{\partial f}{\partial u}\right)$ in the fast dynamics exponential leads to stability of the boundary layer system.

The control problem for the singularly perturbed system is

$$\begin{cases} \dot{\boldsymbol{x}}(\boldsymbol{t}) = \boldsymbol{f}(\boldsymbol{t}, \boldsymbol{x}(\boldsymbol{t}), \boldsymbol{u}(\boldsymbol{t}), \boldsymbol{\epsilon}), \ \boldsymbol{x}(\boldsymbol{0}) = \boldsymbol{\xi}(\boldsymbol{\epsilon}) \\ \boldsymbol{\epsilon}\dot{\boldsymbol{u}} = \ \boldsymbol{g}(\boldsymbol{t}, \boldsymbol{x}(\boldsymbol{t}), \boldsymbol{u}(\boldsymbol{t}), \boldsymbol{\epsilon}), \ \boldsymbol{u}(\boldsymbol{0}) = \boldsymbol{\eta}(\boldsymbol{\epsilon}) \end{cases} \tag{4-1}$$

If the above system is in standard form $g(t, x(t), u(t), 0) = 0$, then we can get $u = h(t, x)$.

If we define $v(t, x) = u - h(t, x)$, then the system

$$\dot{x(t)} = f(t, x(t), h(t, x), 0), \qquad x(0) = \xi(0) = \xi_0$$

is called the reduced system, and the system

$$\frac{dv}{d\tau} = g(t, x(t), v + h(t, x), 0), \qquad v(0) = \eta_0 - h(t, \xi_0)$$

is called the boundary layer system, where the new time scale τ is related to original time t via the relationship $\tau = \frac{t}{\epsilon}$.

Here $g(t, x(t), v + h(t, x), 0)$ can be considered as:

$$\boldsymbol{\frac{dv}{d\tau} = -P^T(t, e(t), z(t), v + h(t, e, z))f\ (t, e, z, v\ +\ h(t, e, z))} \qquad (4\text{-}2)$$

where $e(t) = x_r(t) - x_r^r(t)$, and $x_r^r(t)$ is the desired state variables we want to have. And the dimension of this $x_r^r(t)$ is not the same as the number of state variables. It is equal to the relative degree of the MIMO system, where $z(t)$ denotes the rest of the state variables.

Let the relative degree be "r" then the desired response will have a dynamics as follows:

$$\dot{x_r}(t) = A_r x_r(t) + B_r r(t), \qquad x_r(0) = x_{r0},$$

Then the error dynamics become:

$$\dot{e}(t) = \boldsymbol{F}(e\ +\ xr(t), z, u(t)) - A_r x_r(t) - B_r r(t)$$

and $\boldsymbol{P} \in \mathbb{R}^{mxm}$, where m is the number of inputs, is the Jacobian matrix $\frac{\partial \boldsymbol{F}}{\partial u}$. such that

$$\boldsymbol{P_{ij}}\ (x, z, u)\ = \frac{\partial \boldsymbol{F_i}(x,z,u)}{\partial u_j}$$

According to the theorem given in [17] the controller found by the fast dynamics of equation 4-2 leads to asymptotic stability of the nonlinear nonaffine-in-control system.

Chapter 5
RESULTS AND DISCUSSIONS

Before starting the simulation in 6 DOF model, a reduced order model is simulated in the MATLAB SIMULINK environment. The reduced model consists of 3 degrees of freedom. Those are as follows:

1) Pitch angle ϕ

2) Height of the aircraft z_g

3) Longitudinal Distance of the aircraft from the launching point. x_g

Table 5-1 Initial conditions used in the simulation

Initial velocity [m/s]	0
Initial body attitude [rad]	0
Initial incidence [rad]	0
Initial body rotation rate [rad/sec]	0
Initial position (x z) [m]	[0,0]
Mass [Kg]	1000
Inertia [Kg.m^2]	1000
Acceleration due to gravity [m/s/s]	-9.81

The thrust value given to the aircraft is maintained at 3000 N/m. And the simulation is run for 15 secs.

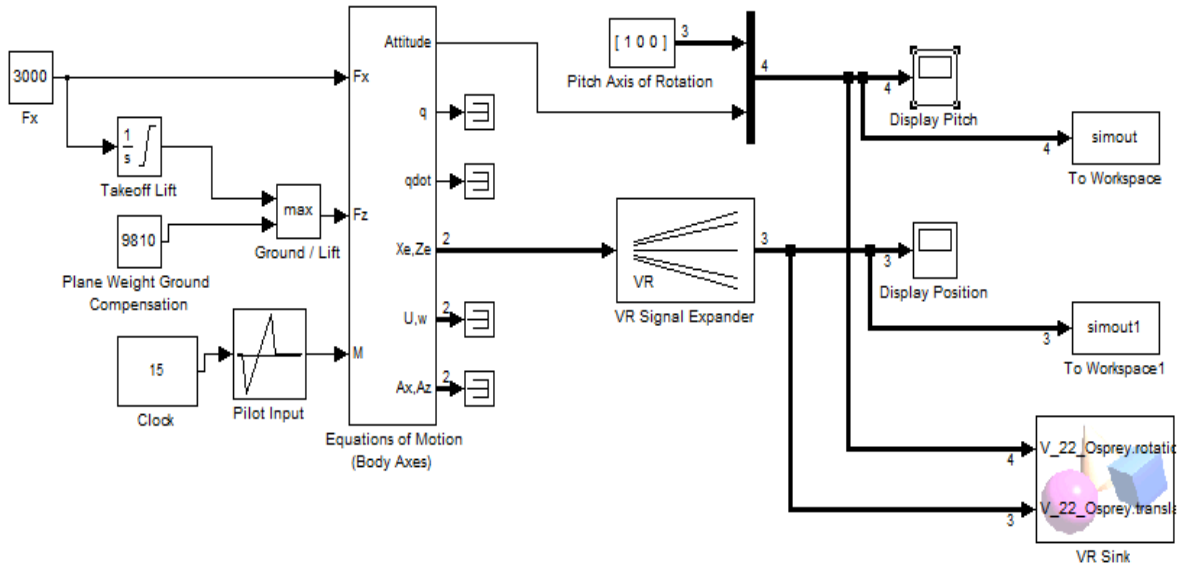

Figure 5-1 3 DoF Model Block Diagram

The output of the simulation are taken out as the 3 state variables. And the state variables were sent to an animation environment. The animation environment is created by the help of VRML (Virtual Reality Modelling Language). The objects were made with the use of the software Cinema 4D. And then they were exported by the vrml file extension. In MATLAB this this file is imported and with the use of video animation tool box the simulation outputs were fed to these objects. The objects created in Cinema 4D include every part of the V 22 Osprey model, viz., nacelles, empennage, fuselage, the runway and the environment.

Animation always gives a visual aid for the analysis of the simulation results. First of all the animation is done by the MATLAB script file coding as shown in . But as the process is a real time one the speed of the animation were not satisfactory. Which was overcame by the use of VRML language.

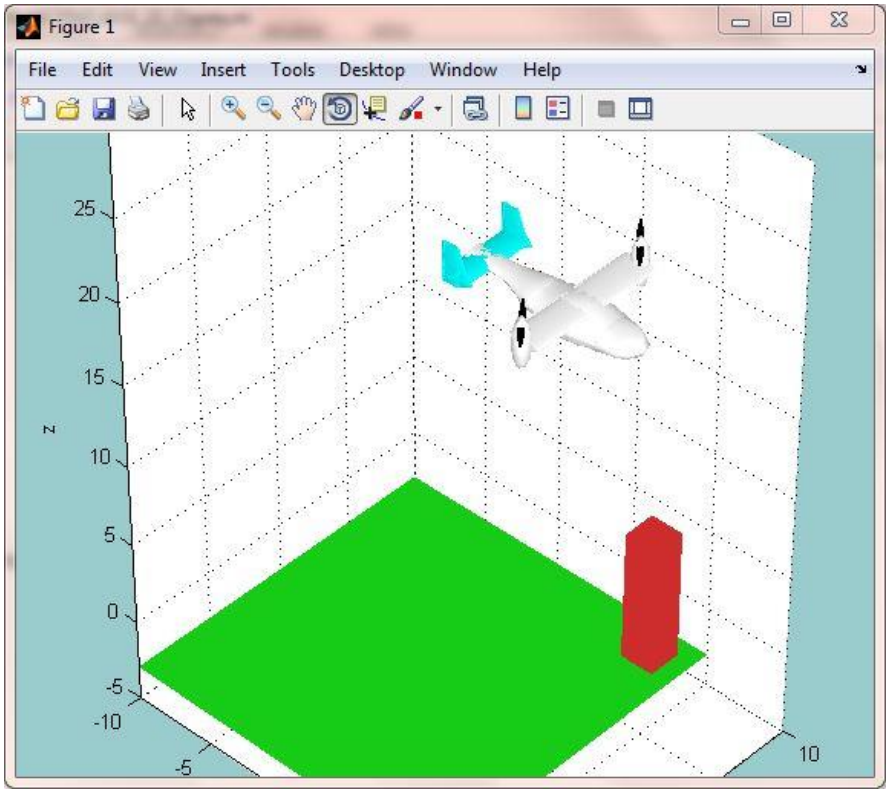

Figure 5-2 Annimation using MATLAB script file coding

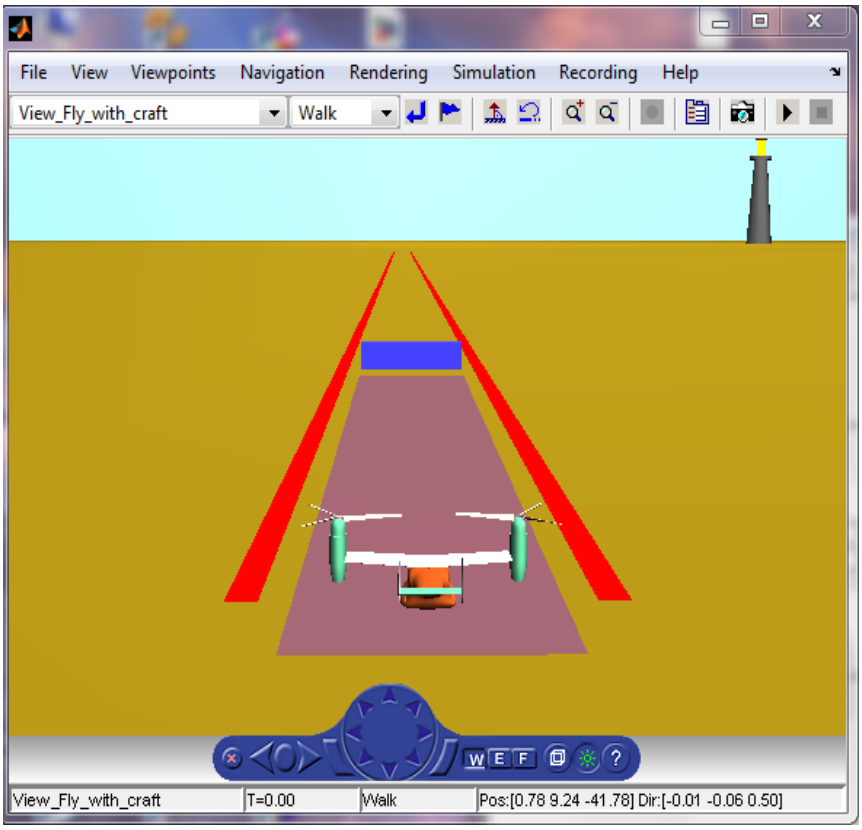

Figure 5-3 Annimation using VRML Language

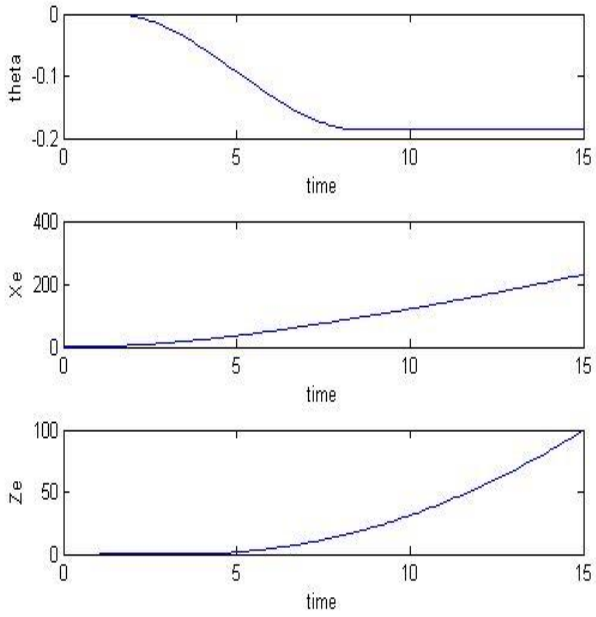

Figure 5-4 Simulation result of the 3 state variables of 3 DoF model

VRML animation responded to the simulation output satisfactorily in real time.

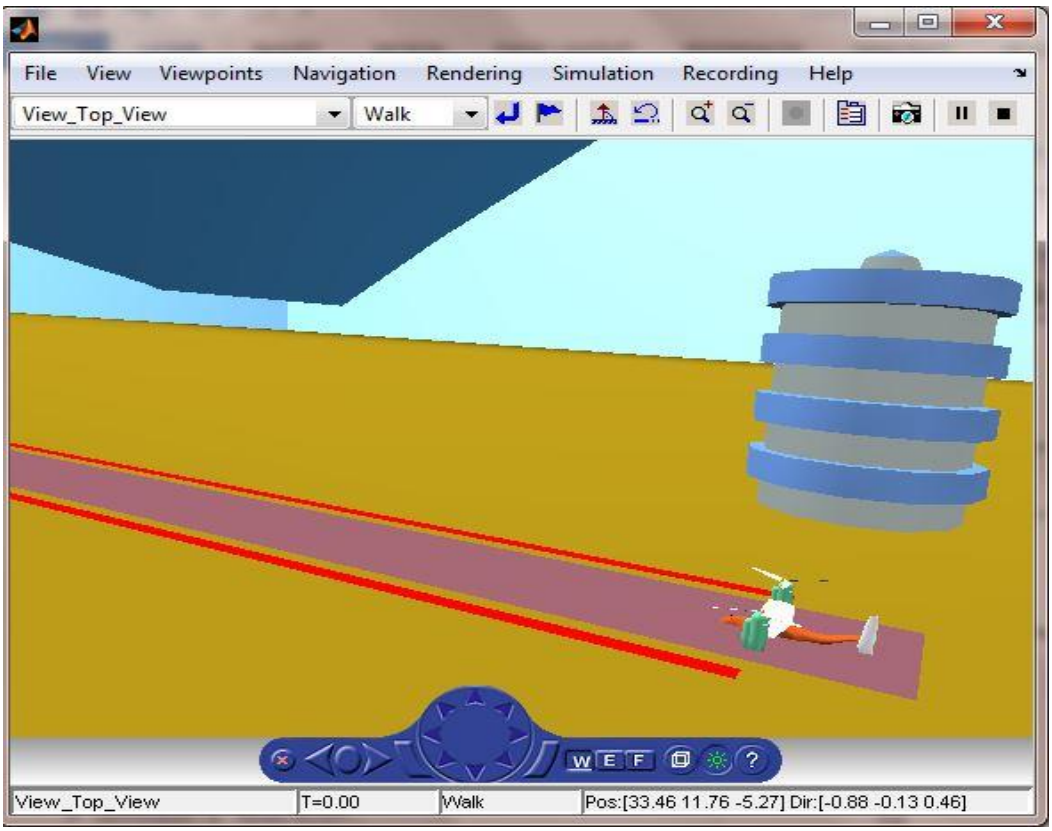

Figure 5-5 Aircraft at its initial Position

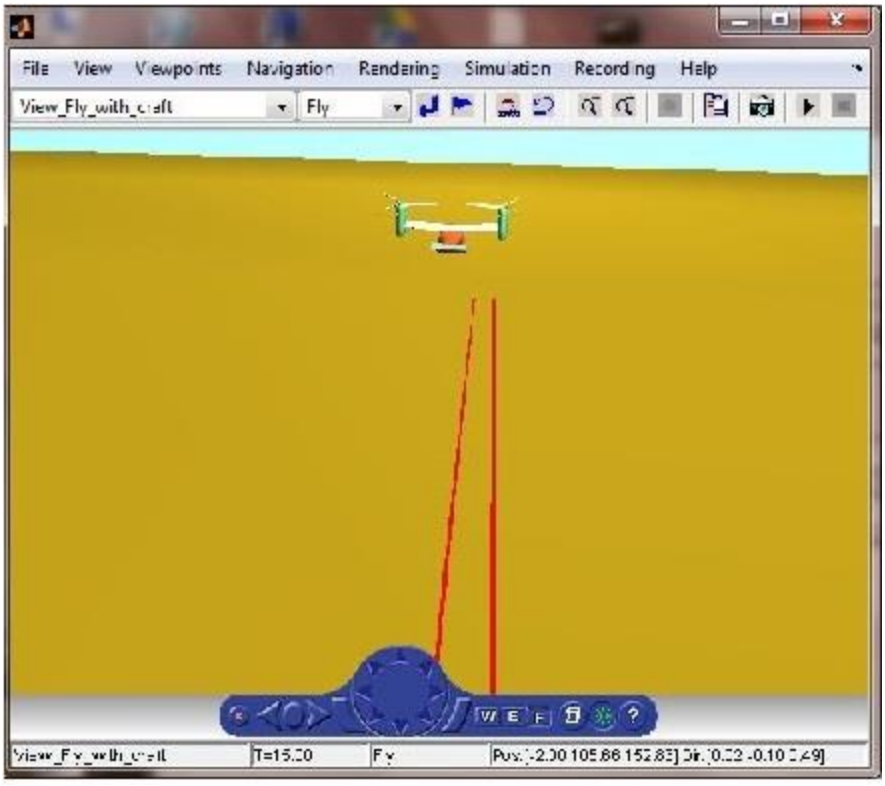

Figure 5-6 Aircraft at its final position

Chapter 6
APPENDICES
APPENDIX- A INERTIA TENSOR

Calculating Inertia Tensor of a Rigid Body

We know angular momentum of a rigid body

$$\boldsymbol{H} = \sum_{\boldsymbol{i}} (\boldsymbol{r_i} \times m_i \boldsymbol{v_i})$$

$$= \sum_{\boldsymbol{i}} m_i \left(\boldsymbol{r_i} \times (\boldsymbol{\omega} \times \boldsymbol{r_i})\right) \ldots\ldots (4.1)$$

We also know that $\boldsymbol{H} = \boldsymbol{I\omega}\ldots\ldots\ldots\ldots (4.2)$

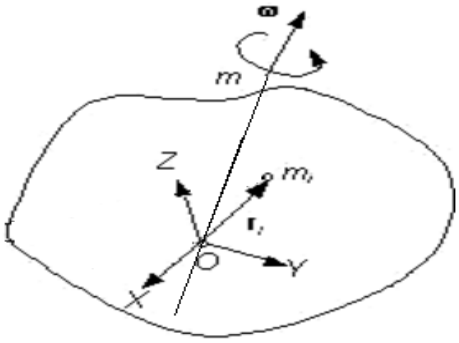

Figure 6-1 Elementary moment of inertia

So from the above two equations we can find inertia tensor $\boldsymbol{I}$ as follows:

$$\sum_{\boldsymbol{i}} m_i \left(\boldsymbol{r_i} \times (\boldsymbol{\omega_i} \times \boldsymbol{r_i})\right) = \sum_{\boldsymbol{i}} m_i \begin{bmatrix} 0 & -z_i & y_i \\ z_i & 0 & -x_i \\ -y_i & x_i & 0 \end{bmatrix} \begin{bmatrix} 0 & -\omega_z & \omega_y \\ \omega_z & 0 & -\omega_x \\ -\omega_y & \omega_x & 0 \end{bmatrix} \begin{bmatrix} x_i \\ y_i \\ z_i \end{bmatrix}$$

$$= \sum_{\boldsymbol{i}} m_i \begin{bmatrix} \omega_x({y_i}^2 + {z_i}^2) & -\omega_y x_i y_i & -\omega_z x_i z_i \\ -\omega_x x_i y_i & \omega_y({z_i}^2 + {x_i}^2) & -\omega_z y_i z_i \\ -\omega_x x_i z_i & -\omega_y y_i z_i & \omega_z({x_i}^2 + {y_i}^2) \end{bmatrix}$$

$$= \begin{bmatrix} \sum_i m_i ({y_i}^2 + {z_i}^2) & -\sum_i m_i x_i y_i & -\sum_i m_i x_i z_i \\ -\sum_i m_i x_i y_i & \sum_i m_i ({z_i}^2 + {x_i}^2) & -\sum_i m_i y_i z_i \\ -\sum_i m_i x_i z_i & -\sum_i m_i y_i z_i & \sum_i m_i ({x_i}^2 + {y_i}^2) \end{bmatrix} \begin{bmatrix} \omega_x \\ \omega_y \\ \omega_z \end{bmatrix}$$

$$= \begin{bmatrix} I_x & -I_{xy} & -I_{xz} \\ -I_{xy} & I_y & -I_{yz} \\ -I_{xz} & -I_{yz} & I_z \end{bmatrix} \begin{bmatrix} \omega_x \\ \omega_y \\ \omega_z \end{bmatrix} = \boldsymbol{I\omega},$$

For continuous body $\sum \rightarrow \int$

So inertial tensor is $\boldsymbol{I} = \begin{bmatrix} I_x & -I_{xy} & -I_{xz} \\ -I_{xy} & I_y & -I_{yz} \\ -I_{xz} & -I_{yz} & I_z \end{bmatrix}$

Transformation of Inertia Tensor

Rotation

The angular momentum of a rigid body rotating about an axis passing through the origin of the local reference frame (frame **A**) is $\boldsymbol{H_A = I_A \omega_A}$**……**(4.3)

Now let's transform this angular momentum vector to another reference frame **B** $\boldsymbol{H_B = {}^B T_A H_A}$**……**(4.4)

Combination of equation (4.3) and (4.4) we get

$$\boldsymbol{H_B = {}^B T_A H_A \omega_A}$$

$$\boldsymbol{\Rightarrow H_B = {}^B T_A H_A \left[\left({}^B T_A \right)^{-1} {}^B T_A \right] \omega_A}$$

$$\boldsymbol{\Rightarrow H_B = \left[{}^B T_A H_A \left({}^B T_A \right)^{-1} \right] \left[{}^B T_A \omega_A \right]}$$

$$\boldsymbol{= I_B \omega_B}$$

So from the above analysis $\boldsymbol{{}^B T_A = {}^B R_A}$, i.e. the Euler transformation matrix of rotation from frame **A** to frame **B.** $\boldsymbol{\omega_B}$ is the angular velocity w.r.t. frame **B.**

The above transformation was for a rotated frame. If the frame is translated then the transformation will be as follow:

Translation

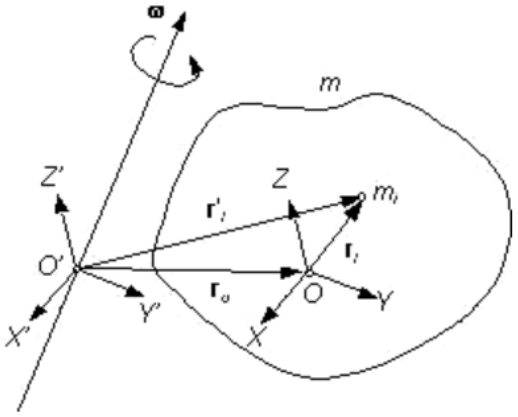

Figure 6-2 Frame translation

This figure shows to reference frames: $Oxyz$ system and the $O'x'y'z'$ system. The xyz is the local reference frame fixed to the body with origin at it's at the body's C.G. The $x'y'z'$ on the other hand is parallel to xyz different origin.

$$\boldsymbol{I'} = \begin{bmatrix} \sum_i m_i \left({y'}_i^2 + {z'}_i^2\right) & -\sum_i m_i\, x'_i y'_i & -\sum_i m_i\, x'_i z'_i \\ -\sum_i m_i\, x'_i y'_i & \sum_i m_i \left({z'}_i^2 + {x'}_i^2\right) & -\sum_i m_i\, y'_i z'_i \\ -\sum_i m_i\, x'_i z'_i & -\sum_i m_i\, y'_i z'_i & \sum_i m_i \left({x'}_i^2 + {y'}_i^2\right) \end{bmatrix}$$

$$\sum_i m_i\, {x'}_i^2 = \sum_i m_i\, (x_o + x_i)^2 = \sum_i m_i\, [{x_o}^2 + 2x_o x_i + {x_i}^2]$$

$$= {x_o}^2 \sum_i m_i + 2x_o \sum_i m_i\, x_i + \sum_i m_i\, {x_i}^2$$

The middle term is zero as O is the C.G. So $\sum_i m_i\, {x'}_i^2 = {x_o}^2 \sum_i m_i + \sum_i m_i\, {x_i}^2$

Similarly $\sum_i m_i\, {y'}_i^2 = {y_o}^2 \sum_i m_i + \sum_i m_i\, {y_i}^2$

And $\sum_i m_i\, {z'}_i^2 = {z_o}^2 \sum_i m_i + \sum_i m_i\, {z_i}^2$

$$\sum_i m_i\, x'_i y'_i = \sum_i m_i\, (x_o + x_i)(y_o + y_i)$$

$$= x_o y_o \sum_i m_i + y_o \sum_i m_i x_i + x_o \sum_i m_i y_i + \sum_i m_i\, x_i y_i$$

Again in the above equation the middle two terms are zero. So

$$\sum_i m_i\, x'_i y'_i = x_o y_o \sum_i m_i + \sum_i m_i\, x_i y_i,$$

Similarly $\sum_i m_i\, y'_i z'_i = y_o z_o \sum_i m_i + \sum_i m_i\, y_i z_i,$

And $\sum_i m_i\, z'_i x'_i = z_o x_o \sum_i m_i + \sum_i m_i\, z_i x_i$

So $\boldsymbol{I' = I_{CG} + I_t}$

And $\boldsymbol{I_t} = \begin{bmatrix} \sum_i m_i\, ({y_o}^2 + {z_o}^2) & -\sum_i m_i\, x_o y_o & -\sum_i m_i\, x_o z_o \\ -\sum_i m_i\, x_o y_o & \sum_i m_i\, ({z_o}^2 + {x_o}^2) & -\sum_i m_i\, y_o z_o \\ -\sum_i m_i\, x_o z_o & -\sum_i m_i\, y_o z_o & \sum_i m_i\, ({x_o}^2 + {y_o}^2) \end{bmatrix}$

So whenever a system is transformed it is rotated 1st to make it parallel to the main reference coordinate system. Then it is translated from to its reference origin.

APPENDIX- B RIGID BODY DYNAMICS

The overall goal of this study is to show that the rigid body kinetics can be expressed in a vectorial setting according to:

$$\boldsymbol{Q} = \mathbb{I}\dot{\boldsymbol{Y}} + \boldsymbol{\Omega}\mathbb{I}\boldsymbol{Y}$$

$\mathbb{I}$ = Rigid body mass/inertia matrix $\in \boldsymbol{R^{6x6}}$

$\boldsymbol{\Omega}$ = Rigid body velocity matrix $\in \boldsymbol{R^{6x6}}$

$\boldsymbol{\Omega}\mathbb{I}$ = Rigid body Coriolis and centripetal matrix due to the rotation of the body-frame about the inertial frame. $\in \boldsymbol{R^{6x6}}$

Body-frame → $\{b\}$, Inertia frame → $\{i\}$,

$\boldsymbol{Y} = [U \quad V \quad W \quad P \quad Q \quad R]^{\boldsymbol{T}}$ = General velocity expressed in $\{b\}$,

$\boldsymbol{Q} = [\mathbb{F}_x \quad \mathbb{F}_y \quad \mathbb{F}_z \quad \mathbb{M}_x \quad \mathbb{M}_y \quad \mathbb{M}_z]^{\boldsymbol{T}}$ = Generalized force expressed in $\{b\}$

The equation of motion will be represented in two body-fixed frames.

1) Center of gravity (C.G.), O_g
2) Origin O_b of $\{b\}$

These points coincide if the vector $\overrightarrow{\boldsymbol{r_g}} = \vec{0}$

The time differentiation of a vector

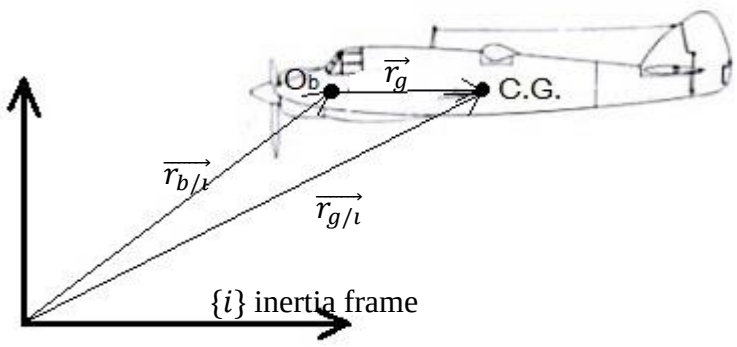

Figure 6-3 Rigid body Reference Points

$\vec{\boldsymbol{a}}$ in the moving reference frame {b} satisfies $\left(\frac{d\vec{\boldsymbol{a}}}{dt}\right)_i = \left(\frac{d\vec{\boldsymbol{a}}}{dt}\right)_b + \vec{\boldsymbol{\omega}}_{\boldsymbol{b/i}} \times \vec{\boldsymbol{a}}$

Time diffentiation in {b} is denoted as $\dot{\vec{\boldsymbol{a}}} = \left(\frac{d\vec{\boldsymbol{a}}}{dt}\right)_b$

Newton-Euler Equation of motion about C.G.

Coordinate free vector: A vector $\vec{\boldsymbol{v}}_{\boldsymbol{b/i}}$, velocity vector of {b} w.r.t {i}, is defined by its magnitude and direction but without reference to a coordinate frame.

Coordinate vector: A vector $\overrightarrow{\boldsymbol{v}^{\boldsymbol{b}}_{\boldsymbol{b/\imath}}}$ decomposed in the inertia reference frame is denoted by $\overrightarrow{\boldsymbol{v}^{\boldsymbol{\imath}}_{\boldsymbol{b/\imath}}}$.

Newton-Euler Formulation

Newton's second law relates mass , acceleration $\dot{\vec{\boldsymbol{v}}}_{\boldsymbol{g/\imath}}$ and the force $\overrightarrow{\mathbb{F}_{\boldsymbol{g}}}$ according to $m\dot{\vec{\boldsymbol{v}}}_{\boldsymbol{g/\imath}} = \overrightarrow{\mathbb{F}_{\boldsymbol{g}}}$ **,** where the subscript **g** denotes the C.G.

Euler's 1st and 2nd axioms, suggest to express Newton's 2nd law in terms of both linear momentum $\overrightarrow{\boldsymbol{P}_{\boldsymbol{g}}}$ and angular momentum $\overrightarrow{\boldsymbol{H}_{\boldsymbol{g}}}$ according to

$$\left(\frac{d\overrightarrow{\boldsymbol{P}_{\boldsymbol{g}}}}{dt}\right)_i = \overrightarrow{\mathbb{F}_{\boldsymbol{g}}}, \;\&\; \overrightarrow{\boldsymbol{P}_{\boldsymbol{g}}} = m\vec{\boldsymbol{v}}_{\boldsymbol{g/i}}$$

$$\left(\frac{d\overrightarrow{\boldsymbol{H}_{\boldsymbol{g}}}}{dt}\right)_i = \overrightarrow{\mathbb{M}_{\boldsymbol{g}}}, \;\&\; \overrightarrow{\boldsymbol{H}_{\boldsymbol{g}}} = \boldsymbol{I}_{\boldsymbol{g}}\vec{\boldsymbol{\omega}}_{\boldsymbol{b/i}}$$

$\overrightarrow{\mathbb{F}_{\boldsymbol{g}}}$ and $\overrightarrow{\mathbb{M}_{\boldsymbol{g}}}$ are the forces and moments about C.G. . $\vec{\boldsymbol{\omega}}_{\boldsymbol{b/i}}$ is the angular velocity of the frame {b} relative to frame {i}. $\boldsymbol{I}_{\boldsymbol{g}}$ is the inertia tensor about the body's C.G.

Translation Motion about C.G.

From Figure 4-3 $\overrightarrow{\boldsymbol{r}_{\boldsymbol{g/\imath}}} = \overrightarrow{\boldsymbol{r}_{\boldsymbol{b/\imath}}} + \overrightarrow{\boldsymbol{r}_{\boldsymbol{g}}}$

The differentiation of $\overrightarrow{\boldsymbol{r_{g/\iota}}}$ in a moving frame $\{b\}$ gives

$$\vec{\boldsymbol{v}}_{\boldsymbol{g/i}} = \vec{\boldsymbol{v}}_{\boldsymbol{b/i}} + \left(\frac{d\overrightarrow{\boldsymbol{r_g}}}{dt}\right)_b + \vec{\boldsymbol{\omega}}_{\boldsymbol{b/i}} \times \overrightarrow{\boldsymbol{r_g}}$$

For a rigid body, $\left(\frac{d\overrightarrow{r_g}}{dt}\right)_b = 0.$

$$\vec{\boldsymbol{v}}_{\boldsymbol{g/i}} = \vec{\boldsymbol{v}}_{\boldsymbol{b/i}} + \vec{\boldsymbol{\omega}}_{\boldsymbol{b/i}} \times \overrightarrow{\boldsymbol{r_g}}$$

$$\overrightarrow{\mathbb{F}_{\boldsymbol{g}}} = \left(\frac{dm\vec{\boldsymbol{v}}_{\boldsymbol{g/i}}}{dt}\right)_i = m\left(\dot{\vec{\boldsymbol{v}}}_{\boldsymbol{g/\iota}} + \vec{\boldsymbol{\omega}}_{\boldsymbol{b/i}} \times \vec{\boldsymbol{v}}_{\boldsymbol{g/i}}\right)$$

The cross product can be converted to a matrix multiplication by representing vector $\vec{\boldsymbol{\omega}}_{\boldsymbol{b/i}}$ in a skew symmetric matrix $\boldsymbol{S}\left(\boldsymbol{\omega}_{\boldsymbol{b/i}}\right)$

$$\boldsymbol{S}\left(\boldsymbol{\omega}_{\boldsymbol{b/i}}\right) = \begin{bmatrix} 0 & -\omega_z & \omega_y \\ \omega_z & 0 & -\omega_x \\ -\omega_y & \omega_x & 0 \end{bmatrix}$$

If we represent $\vec{\boldsymbol{\omega}}_{\boldsymbol{b/i}}$ in the body-frame the vector will be same but the basis vector will be different.

$$\boldsymbol{S}\left(\boldsymbol{\omega}^{\boldsymbol{b}}_{\boldsymbol{g/i}}\right) = \begin{bmatrix} 0 & -R & Q \\ R & 0 & -P \\ -Q & P & 0 \end{bmatrix}$$

So the translational motion about C.G. expressed in $\{b\}$

$$\overrightarrow{\mathbb{F}_{\boldsymbol{g}}} = m\left(\dot{\overrightarrow{\boldsymbol{v}^{\boldsymbol{b}}_{\boldsymbol{g/\iota}}}} + \boldsymbol{S}\left(\boldsymbol{\omega}^{\boldsymbol{b}}_{\boldsymbol{g/i}}\right)\overrightarrow{\boldsymbol{v}^{\boldsymbol{b}}_{\boldsymbol{g/\iota}}}\right)$$

Rotational Motion about C.G.

The derivation starts with Euler's 2nd axiom.

$$\overrightarrow{\mathbb{M}_{\boldsymbol{g}}} = \left(\frac{d\boldsymbol{I}_{\boldsymbol{g}}\vec{\boldsymbol{\omega}}_{\boldsymbol{g/i}}}{dt}\right)_i = \boldsymbol{I}_{\boldsymbol{g}}\dot{\overrightarrow{\boldsymbol{\omega}^{\boldsymbol{b}}_{\boldsymbol{g/\iota}}}} + \overrightarrow{\boldsymbol{\omega}^{\boldsymbol{b}}_{\boldsymbol{b/\iota}}} \times \boldsymbol{I}_{\boldsymbol{g}}\overrightarrow{\boldsymbol{\omega}^{\boldsymbol{b}}_{\boldsymbol{g/\iota}}}$$

$$= \boldsymbol{I_g}\dot{\overrightarrow{\boldsymbol{\omega}^{\boldsymbol{b}}_{\boldsymbol{g/\iota}}}} + \boldsymbol{S}\left(\boldsymbol{\omega}^{\boldsymbol{b}}_{\boldsymbol{g/i}}\right)\boldsymbol{I_g}\overrightarrow{\boldsymbol{\omega}^{\boldsymbol{b}}_{\boldsymbol{g/\iota}}}$$

Equations of Motion about C.G.

$$\boldsymbol{Q_g} = \mathbb{I}_{\boldsymbol{g}}\dot{\boldsymbol{Y}}_{\boldsymbol{g}} + \boldsymbol{\Omega_g}\mathbb{I}_{\boldsymbol{g}}\boldsymbol{Y_g}$$

$$\begin{bmatrix}\overrightarrow{\mathbb{F}^{\boldsymbol{b}}_{\boldsymbol{g}}}\\ \overrightarrow{\mathbb{M}^{\boldsymbol{b}}_{\boldsymbol{g}}}\end{bmatrix} = \begin{bmatrix}m\mathbf{I}_{3\times3} & \mathbf{0}_{3\times3}\\ \mathbf{0}_{3\times3} & \boldsymbol{I_g}\end{bmatrix}\begin{bmatrix}\dot{\overrightarrow{\boldsymbol{v}^{\boldsymbol{b}}_{\boldsymbol{g/\iota}}}}\\ \dot{\overrightarrow{\boldsymbol{\omega}^{\boldsymbol{b}}_{\boldsymbol{g/\iota}}}}\end{bmatrix} + \begin{bmatrix}\boldsymbol{S}\left(\boldsymbol{\omega}^{\boldsymbol{b}}_{\boldsymbol{b/i}}\right) & \mathbf{0}_{3\times3}\\ \mathbf{0}_{3\times3} & \boldsymbol{S}\left(\boldsymbol{\omega}^{\boldsymbol{b}}_{\boldsymbol{b/i}}\right)\end{bmatrix}\begin{bmatrix}m\mathbf{I}_{3\times3} & \mathbf{0}_{3\times3}\\ \mathbf{0}_{3\times3} & \boldsymbol{I_g}\end{bmatrix}\begin{bmatrix}\overrightarrow{\boldsymbol{v}^{\boldsymbol{b}}_{\boldsymbol{g/\iota}}}\\ \overrightarrow{\boldsymbol{\omega}^{\boldsymbol{b}}_{\boldsymbol{g/\iota}}}\end{bmatrix}$$

Newton Euler Equations About Body-frame Origin

From an aircraft point of view it is desirable to derive the equations of motion for an arbitrary origin to take the advantage of aircraft's geometric properties. Since the aerodynamic forces and moments often are computed in that origin, Newton's law will be formulated in the suitable body-frame origin as well.

Transformation of equation from C.G. to O_b is done using coordinate transformation.

$$\overrightarrow{\boldsymbol{v}^{\boldsymbol{b}}_{\boldsymbol{g/\iota}}} = \overrightarrow{\boldsymbol{v}^{\boldsymbol{b}}_{\boldsymbol{b/\iota}}} + \overrightarrow{\boldsymbol{\omega}^{\boldsymbol{b}}_{\boldsymbol{b/\iota}}} \times \overrightarrow{\boldsymbol{r}^{\boldsymbol{b}}_{\boldsymbol{g}}} = \overrightarrow{\boldsymbol{v}^{\boldsymbol{b}}_{\boldsymbol{b/\iota}}} - \overrightarrow{\boldsymbol{r}^{\boldsymbol{b}}_{\boldsymbol{g}}} \times \overrightarrow{\boldsymbol{\omega}^{\boldsymbol{b}}_{\boldsymbol{b/\iota}}} = \overrightarrow{\boldsymbol{v}^{\boldsymbol{b}}_{\boldsymbol{b/\iota}}} - \boldsymbol{S}\left(\boldsymbol{r}^{\boldsymbol{b}}_{\boldsymbol{g}}\right)\overrightarrow{\boldsymbol{\omega}^{\boldsymbol{b}}_{\boldsymbol{b/\iota}}}$$

For a skew symmetric matrix $-\boldsymbol{S}\left(\boldsymbol{r}^{\boldsymbol{b}}_{\boldsymbol{g}}\right) = \boldsymbol{S}^{\boldsymbol{T}}\left(\boldsymbol{r}^{\boldsymbol{b}}_{\boldsymbol{g}}\right)$

So $\overrightarrow{\boldsymbol{v}^{\boldsymbol{b}}_{\boldsymbol{g/\iota}}} = \overrightarrow{\boldsymbol{v}^{\boldsymbol{b}}_{\boldsymbol{b/\iota}}} + \boldsymbol{S}^{\boldsymbol{T}}\left(\boldsymbol{r}^{\boldsymbol{b}}_{\boldsymbol{g}}\right)\overrightarrow{\boldsymbol{\omega}^{\boldsymbol{b}}_{\boldsymbol{b/\iota}}}$, and

$\begin{bmatrix}\boldsymbol{v}^{\boldsymbol{b}}_{\boldsymbol{g/i}}\\ \boldsymbol{\omega}^{\boldsymbol{b}}_{\boldsymbol{g/i}}\end{bmatrix} = \boldsymbol{T}(\boldsymbol{r}^{\boldsymbol{b}}_{\boldsymbol{g}})\begin{bmatrix}\boldsymbol{v}^{\boldsymbol{b}}_{\boldsymbol{b/i}}\\ \boldsymbol{\omega}^{\boldsymbol{b}}_{\boldsymbol{b/i}}\end{bmatrix}$, $\boldsymbol{\omega}^{\boldsymbol{b}}_{\boldsymbol{g/i}} = \boldsymbol{\omega}^{\boldsymbol{b}}_{\boldsymbol{b/i}}$ ($\because$ The frame is only translated from O_g to O_b)

Translation Matrix $\boldsymbol{T}\left(\boldsymbol{r}^{\boldsymbol{b}}_{\boldsymbol{g}}\right) = \begin{bmatrix}\mathbf{I}_{3\times3} & \boldsymbol{S}^{\boldsymbol{T}}\left(\boldsymbol{r}^{\boldsymbol{b}}_{\boldsymbol{g}}\right)\\ \mathbf{0}_{3\times3} & \mathbf{I}_{3\times3}\end{bmatrix}$, and $\boldsymbol{T}^{\boldsymbol{T}}\left(\boldsymbol{r}^{\boldsymbol{b}}_{\boldsymbol{g}}\right) = \begin{bmatrix}\mathbf{I}_{3\times3} & \mathbf{0}_{3\times3}\\ \boldsymbol{S}\left(\boldsymbol{r}^{\boldsymbol{b}}_{\boldsymbol{g}}\right) & \mathbf{I}_{3\times3}\end{bmatrix}$

$$\begin{bmatrix} \overrightarrow{\mathbb{F}_g^b} \\ \overrightarrow{\mathbb{M}_g^b} \end{bmatrix} = \mathbb{I}_g \begin{bmatrix} \dot{\overrightarrow{v_{g/\iota}^b}} \\ \dot{\overrightarrow{\omega_{g/\iota}^b}} \end{bmatrix} + \boldsymbol{\Omega_g} \mathbb{I}_g \begin{bmatrix} \overrightarrow{v_{g/\iota}^b} \\ \overrightarrow{\omega_{g/\iota}^b} \end{bmatrix}$$

$$\Longrightarrow \boldsymbol{T^T} \begin{bmatrix} \overrightarrow{\mathbb{F}_g^b} \\ \overrightarrow{\mathbb{M}_g^b} \end{bmatrix} = \boldsymbol{T^T} \mathbb{I}_g \boldsymbol{T} \begin{bmatrix} \dot{\overrightarrow{v_{b/\iota}^b}} \\ \dot{\overrightarrow{\omega_{b/\iota}^b}} \end{bmatrix} + \boldsymbol{T^T \Omega_g} \mathbb{I}_g \boldsymbol{T} \begin{bmatrix} \overrightarrow{v_{g/\iota}^b} \\ \overrightarrow{\omega_{b/\iota}^b} \end{bmatrix}, \text{ here } \boldsymbol{T} = \boldsymbol{T}\left(\boldsymbol{r_g^b}\right) \text{ as } \boldsymbol{r_g^b} \text{ is constant.}$$

$\boldsymbol{T^T} \mathbb{I}_g \boldsymbol{T} = \mathbb{I}_b$ = Inertia matrix of rigid body w.r.t frame {b}

$$\boldsymbol{T^T \Omega_g} \mathbb{I}_g \boldsymbol{T} = \boldsymbol{T^T \Omega_g} \left(\boldsymbol{T^{T^{-1}} T^T}\right) \mathbb{I}_g \boldsymbol{T} = \left(\boldsymbol{T^T \Omega_b T^{T^{-1}}}\right) \left(\boldsymbol{T^T} \mathbb{I}_g \boldsymbol{T}\right)$$
$$= \boldsymbol{\Omega_b} \mathbb{I}_b$$

Velocity matrix w.r.t frame {b}= $\boldsymbol{\Omega_b} = \begin{bmatrix} \boldsymbol{S}\left(\boldsymbol{\omega_{b/i}^b}\right) & \boldsymbol{0_{3\times 3}} \\ \boldsymbol{S}\left(\overrightarrow{\boldsymbol{r_g^b}} \times \overrightarrow{\boldsymbol{\omega_{b/i}^b}}\right) & \boldsymbol{S}\left(\boldsymbol{\omega_{b/i}^b}\right) \end{bmatrix}$

$\boldsymbol{T^T} \begin{bmatrix} \overrightarrow{\mathbb{F}_g^b} \\ \overrightarrow{\mathbb{M}_g^b} \end{bmatrix} = \begin{bmatrix} \overrightarrow{\mathbb{F}_b^b} \\ \overrightarrow{\mathbb{M}_b^b} \end{bmatrix}$ = Forces and moments acting on the rigid body w.r.t. frame {b}.

Equations of Motion about The body-frame reference

$$\boldsymbol{Q_b} = \mathbb{I}_b \dot{\boldsymbol{Y}}_b + \boldsymbol{\Omega_b} \mathbb{I}_b \boldsymbol{Y_b}$$

REFERENCES

[1] Thanan Yomchinda, "*Integrated Flight Control Design and Handling Qualities Analysis For a Tiltrotor Aircraft*", PhD Thesis, Department of Aerospace Engineering, The Pennsylvania State University,2009

[2] Mark B. Tischler, "*System Identification Methods for Aircraft Flight Control Development and Validation*", Aero flight dynamics Directorate, U.S. Army ATCOM, Ames Research Center, Moffett Field, California, 1995

[3] *Sergey Khantis. "Control System Design Using Evolutionary Algorithms for Autonomous Shipboard Recovery of Unmanned Aerial Vehicles*". PhD thesis, RMIT University, Australia, 2006.

[4] Maisel, M. D., Giulianetti, D. J., Dugan, D. C.: "T*he History of the XV-15 Tilt Rotor Research Aircraft – From Concept to Flight*", NASA, SP-2000-4517, 2000

[5] Horn, J.F. and Bridges, D.O., "*A Model Following Controller Optimized for Gust Rejection during Shipboard Operations*", American Helicopter Society 63rd Annual Forum, 1-3 May 2007.

[6] Calise, A.J. and Rysdyk,R.T., "*Adaptive Model Inversion Flight Control for Tiltrotor Aircraft.*" AIAA Guidance, Navigation and Control Conference, August 1997, Paper No.97-3758.

[7] Calise, A.J., Rysdyk, R.T. and Chen, R. T. N., "*Nonlinear Adaptive Control of Tiltrotor Aircraft Using Neural Networks.*" SAE World Aviation Congress 1997 proceedings, October 1997, Paper No.97-5613.

[8] Calise, A.J. and Rysdyk,R.T., "*Research in Nonlinear Flight Control for Tiltrotor Aircraft Operating in the Terminal Area*." NASA NCC-2-922, November 1996.

[9] Walker, D.J. and Voskuijl, M., "*Active Control of Flight Path and Critical Loads in Tilt-Rotor Aircraft*", American Helicopter Society 63rd Annual Forum, 2007.

[10] Zamri Omar, "*Intelligent Control of a Ducted-Fan VTOL UAV with Conventional Control Surfaces*", PhD Thesis, Department of Aerospace Engineering, RMIT University, 2010

[11] http://www.airforce-technology.com/projects/predator-uav/

[12] http://www.navy.mil/navydata/fact_display.asp?cid=1100&tid=2100&ct=1

[13] http://www.army-technology.com/projects/hunter/

[14] http://www.defenseindustrydaily.com/global-hawk-uav-prepares-for-maritime-role-updated-01218/

[15] http://www.gyrodynehelicopters.com/qh-50_evolution.htm

[16] H.K. Khalil. *Nonlinear Systems*. Prentice Hall, 2002.

[17] Naira Hovakimyan, "*Dynamic Inversion of Multi-input Nonaffine Systems via Time-scale Separation*", Proceedings of the 2006 American Control Conference, Minneapolis, Minnesota, USA, June 14-16, 2006